Endocrine System

6

Saud A. Alenezi and Abdelhamid H. Elgazzar

6.1 The Thyroid Gland

6.1.1 Anatomical and Physiological Considerations

6.1.1.1 Anatomy

The thyroid gland develops from the foramen cecum of the tongue, to which it is connected by the thyroglossal duct. It descends during fetal life to reach the anterior neck by about the seventh week. Absent or aberrant descent results in ectopic locations, including the sublingual region and superior mediastinum.

The normal adult thyroid gland weighs 14–19 g. It is generally smaller in women than in men, and is barely palpable [1, 2]. The thyroid is located in the mid to lower anterior neck, with the isthmus in front of the trachea, usually just below the cricoid cartilage, and the lobes on the sides of the trachea (Fig. 6.1). In older individuals with shorter necks, the thyroid may lie at or just above the suprasternal notch, and it may often be partly substernal. The thyroid gland moves cephalad during swallowing, a characteristic that aids in palpation and in distinction of thyroid from nonthyroid neck masses.

6.1.1.2 Physiology

The thyroid gland regulates a spectrum of physiological activities such as growth, metabolism, homeostasis, and cell proliferation and differentiation through the secretion of thyroid hormones. The thyroid follicle consists of a colloid center, which acts as a storage site for thyroid hormone, surrounded by epithelial cells (Fig. 6.2). The thyroid epithelial cell has a transport mechanism, also referred to as trapping, that enables thyroid concentration of iodide. The sodium-dependent iodide transport activity of the thyroid gland is mainly attributed to the functional expression of the Na^+/I^- Symporter (NIS) localized at the basolateral membrane of thyroid epithelial cells. Symporter activity is influenced primarily by pituitary thyroid-stimulating hormone (TSH), which increases the transport of iodide. The trapped iodide subsequently undergoes organification and incorporation into thyroid hormones.

Additionally, other anions, such as pertechnetate, thiocyanate, and perchlorate, are also accumulated by the thyroid gland. The uptake of pertechnetate is the basis for ^{99m}Tc-pertechnetate scintigraphy. Thiocyanate, derived from certain foods, decreases thyroid accumulation of iodine and may exacerbate iodine deficiency. Perchlorate has diagnostic and therapeutic applications.

Synthesis of hormone takes place in thyroglobulin, a glycoprotein, which is produced in the thyroid cell and extruded into the colloid. Iodine combines with tyrosine in thyroglobulin to form

S. A. Alenezi (✉) · A. H. Elgazzar
Department of Nuclear Medicine, Faculty of Medicine, Kuwait University, Kuwait City, Kuwait

A. H. Elgazzar (ed.), *The Pathophysiologic Basis of Nuclear Medicine*,
https://doi.org/10.1007/978-3-030-96252-4_6

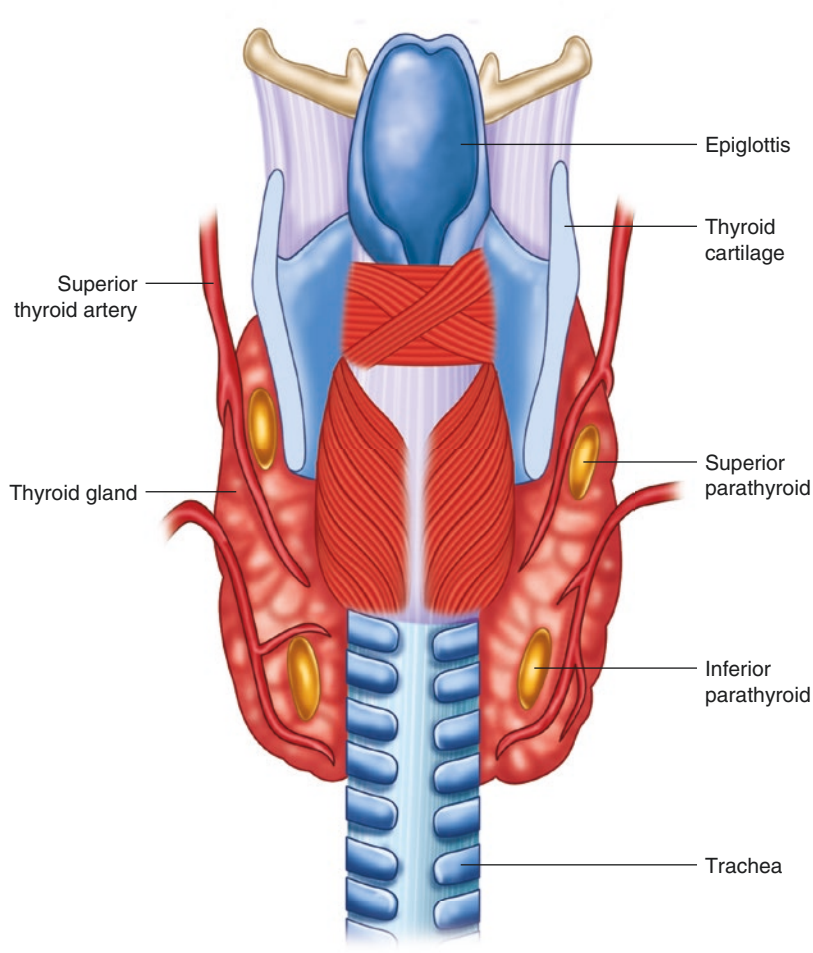

Fig. 6.1 Diagram showingtypical locations of the thyroid and parathyroid glands in the neck

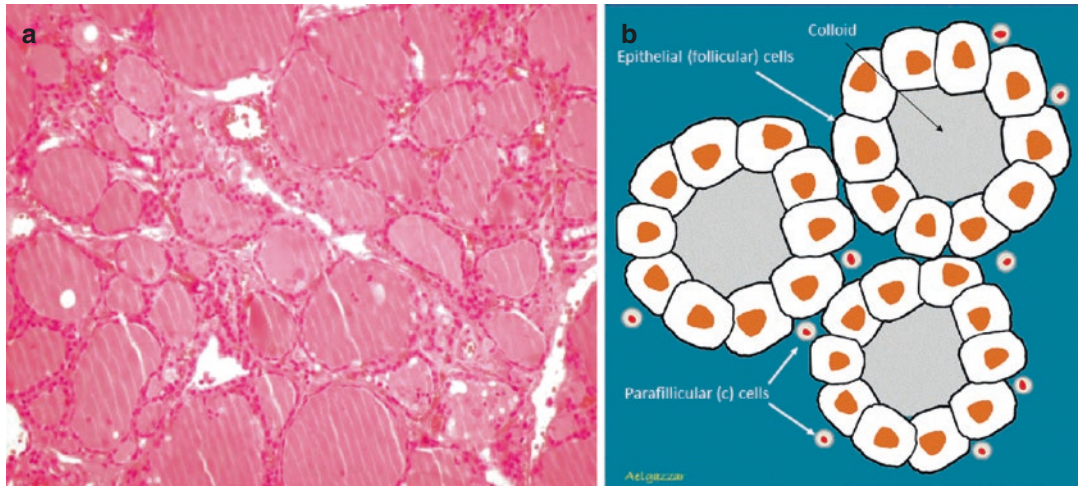

Fig. 6.2 Thyroid follicle. (**a**) Low-power field images of thyroid gland tissue showing the follicles lined by follicular cells and filled with colloid. (**b**) Diagram illustrating thyroid follicles and cells

Table 6.1 Actions and uses of antithyroid drugs

Drug	Mechanism	Uses
Propylthiouracil (PTU)	Blocks iodine organification	Controls hyperthyroidism in Graves' disease and toxic nodular goiter
	Decreases the monodeiodination of T_4 to T_3	
	Decreases in serum levels of thyrotropin receptor autoantibodies	
Methimazole	Blocks iodine organification	Controls hyperthyroidism in Graves' disease and toxic nodular goiter
	Decreases in serum levels of thyrotropin receptor autoantibodies	
Glucocorticoids	Rapid inhibitory effect on peripheral conversion of T_4 to T_3	Thyroid storm, Graves' ophthalmopathy, and protracted subacute thyroiditis
Iodides	Decreases synthesis of thyroid hormones	Thyroid storm
Lithium	Blocks release of thyroid hormone	Adjunct in treatment of severe hyperthyroidism
Potassium perchlorate	Decreases thyroid iodine uptake and discharges unbound iodine	Amiodarone-induced thyroid dysfunction and after accidental exposure to radioactive iodine

monoiodotyrosine (MIT) and diiodotyrosine (DIT). Subsequently, the iodotyrosines are coupled, with the formation of thyroxine (T_4) and triiodothyronine (T_3). The coupling reaction also is mediated by peroxidase.

Release of thyroid hormones occurs in response to TSH, where a small amount of colloid is engulfed by the epithelial cell and proteolyzed, with release of T_3 and T_4, which diffuse into the circulation. Thyroglobulin not undergoing proteolysis also enters the circulation in small quantities. The serum thyroglobulin has been used as a tumor marker in differentiated thyroid cancer. Thyroglobulin decreases and eventually becomes undetectable following thyroidectomy and ^{131}I ablation, and its subsequent rise indicates a recurrence. TSH stimulation, by promoting colloid endocytosis, increases the amount of thyroglobulin released. Consequently, the serum thyroglobulin is a more reliable tumor marker at high TSH levels [3, 4].

Most of the circulating thyroid hormones are bound to plasma proteins, the free fraction comprising about 0.05% of T_4 and 0.2% of T_3. Only the free hormone has metabolic effects, and it is a more accurate measure of thyroid function than the total hormone, which varies with plasma proteins levels. T_3 is considered the active hormone. About 20–30% of the circulating T_3 is secreted by the thyroid gland and the remainder is produced by monodeiodination of T_4 in extrathyroid tissues, notably the liver, kidney, brain, and pituitary [4]. Decrease in the peripheral conversion of T_4 to T_3 is a basis for the use of some antithyroid drugs.

Most antithyroid drugs generally block one or more steps in the synthesis and metabolism of thyroid hormone (Table 6.1). The thiourea derivatives (thionamides), including propylthiouracil (PTU) and methimazole, are the most common antithyroid agents in use [5, 6]. Methimazole is generally the preferred drug since PTU may be associated with serious hepatotoxicity [6]. Other drugs used for their antithyroid actions include glucocorticoids, iodides, lithium, and potassium perchlorate [4].

Thyrotropin-releasing hormone (TRH), a tripeptide originating from the hypothalamic median eminence, stimulates the secretion and synthesis of thyroid-stimulating hormone (TSH, thyrotropin), a glycoprotein, by the anterior pituitary. It increases the transport of iodide, synthesis of hormone, and release of T_3, T_4, and thyroglobulin. The production and release of TSH are influenced by the concentration of T_3 within the pituitary. When the T_3 concentration falls below a set point, TSH secretion increases, and synthesis and release of thyroid hormones are accelerated. Conversely, when the T_3 level rises above the set point, TSH release is inhibited. In addition to its pituitary effect, T_3 inhibits hypothalamic TRH release. Other mechanisms

reported more recently include the inhibitory actions of the released TSH on TRH secretion, and on TSH receptors in the pituitary itself.

In addition to regulation of thyroid function, TSH promotes thyroid growth. If thyroid hormone synthesis is chronically impaired, as in iodine deficiency and autoimmune thyroid disease, chronic TSH stimulation eventually may lead to the development of a goiter.

The serum TSH is a sensitive and specific marker of thyroid function. Normal serum TSH is about 0.45–4.5 μunits/ml, and levels up to 20 μunits/ml are considered normal in newborns because of the contribution of maternal TSH. Serum TSH is increased in primary hypothyroidism and decreased in hyperthyroidism of all etiologies except for the uncommon entity of thyrotropin-induced hyperthyroidism.

The TSH secretion is suppressed by exogenous thyroid hormone to avoid stimulation of tumor growth in patients with differentiated thyroid cancer, and to decrease thyroid size or arrest thyroid growth in the early stages of goiter development.

Stimulation with TSH increases thyroid function and thyroid uptake of radioiodine. This principle is used in differentiated thyroid cancer for the detection and treatment of thyroid remnants and thyroid cancer metastases with radioiodine [6, 7]. Thyroid-stimulating hormone levels are allowed to rise to 30–50 μunits/ml or higher after withholding thyroid hormone supplements, or after administering recombinant human TSH. The latter is becoming popular since it shortens the preparation time and avoids a period of hypothyroidism after stopping thyroid hormone replacement therapy [8, 9]. In thyroid cancer, recombinant TSH is used in diagnosis, monitoring of serum thyroglobulin, and for radioiodine ablation of thyroid remnants after thyroidectomy. FDG PET is optimal at high TSH levels, and it may be combined with radioiodine imaging and thyroglobulin measurement in selected patients [10, 11]. In addition, FDG uptake was found to be of value in identifying metastases in postoperative differentiated thyroid cancer patients and in predicting iodine avidity since SUV higher than four indicate more aggressive disease and higher probability of non-avidity to radioiodine [12].

6.1.1.3 Role of Iodine Metabolism in Thyroid Physiology

Iodine is needed for the production of thyroid hormones. Since the body does not make iodine, it is an essential part of diet. The mean daily turnover of iodine by the thyroid is approximately 60–95 μg in adults in iodine-sufficient areas. The body of a healthy adult contains from 15 to 20 mg of iodine, 70–80% of which is in the thyroid. Iodine is a trace element that is ingested in several chemical forms. Most forms of iodine are reduced to iodide in the gut. Iodide is nearly completely absorbed in the stomach and duodenum [13]. In the basolateral membrane of the thyroid cell, the sodium/iodine symporter transfers iodide into the thyroid across a concentration gradient 20–50 times that of plasma by active transport [13]. Iodine is cleared from the circulation primarily by the thyroid and kidney. Under normal circumstances, plasma iodine has a half-life of approximately 10 h, but this is shortened if the thyroid is overactive, as in iodine deficiency or hyperthyroidism.

Degradation of T_4 and T_3 in the peripheral tissues releases iodine that re-enters the plasma iodine pool. Most ingested iodine is eventually excreted in the urine. Only a small amount appears in the feces.

The mammary glands concentrate iodine and secrete it into breast milk to provide it for the newborn. The salivary glands, gastric mucosa, and choroid plexus also take up small amounts of iodine. The iodine symporter have been reported in trophoblasts, and the placental iodine content is approximately 3% that of the thyroid [14, 15].

Effect of Iodine Insufficiency

Iodine is an essential micronutrient, as it is an integral part of the thyroid hormones thyroxine (T_4) and triiodothyronine (T_3). Severe iodine deficiency results in depleted iodine stores and a failure to sustain normal thyroid hormone levels [16]. The recommended daily intake of iodide is 150 μg for adolescents and adults, and 250 μg in pregnancy and lactation [17].

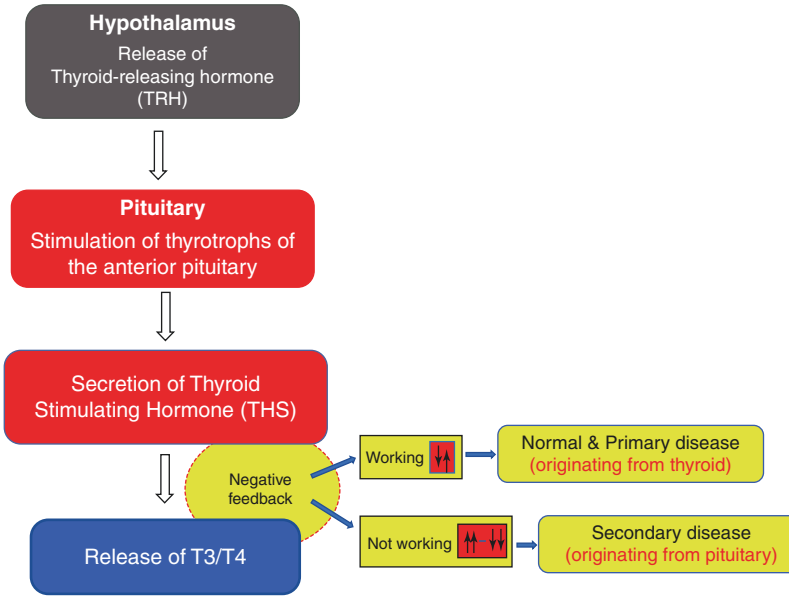

Fig. 6.3 Simple illustration of different hormones related to thyroid function

Reduced synthesis of thyroid hormone is compensated, at least in part, by increased TSH secretion, resulting eventually in goiter formation.

Because an adequate supply of thyroid hormone is needed for fetal neurological development, maternal and fetal hypothyroidism resulting from iodine deficiency is associated with varying degrees of neuropsychological deficits including cretinism.

Effect of Excessive Iodine

When intrathyroid iodine concentrations are significantly increased, the rate of thyroid hormone synthesis is decreased, with a reduction in iodothyronine synthesis and decrease in the DIT/MIT ratio. This response is referred to as the Wolff–Chaikoff effect.

Continued exposure to large amounts of iodine would eventually lead to hypothyroidism, with compensatory increase in TSH and development of goiter. While this does occur occasionally, adaptation or escape from the effects of chronic iodide excess is more likely. The inhibitory effect of iodides on thyroid function is utilized clinically for prompt control of severe hyperthyroidism and thyroid storm. In Graves' disease, large doses of iodide decrease not only hormone synthesis but also hormone release [12]. Since escape from the inhibitory effect is likely, iodide therapy is only a short-term measure for lowering thyroid hormone levels rapidly.

Iodine excess may lead to hyperthyroidism or hypothyroidism [13, 14]. Iodine-induced hyperthyroidism, referred to as Jod-Basedow, characteristically occurs in persons with hyperplastic thyroid glands. Hyperthyroidism occurring after iodine supplementation in endemic goiter areas is a classical example. Iodine-containing medical products, including amiodarone, radiographic dyes, and kelp, also have the potential to cause Jod-Basedow [18, 19]. Amiodarone, a cardiac antiarrhythmic drug, is a benzofuranic product with a very high iodine content and may be associated with either hypo- or hyperthyroidism development.

Figure 6.3 summarizes the mechanism of hormonal interactions related to thyroid gland.

6.1.2 Radiopharmaceuticals for Thyroid Imaging

6.1.2.1 Technetium-99m-Pertechnetate

Technetium-99m-pertechnetate is widely used for imaging the thyroid gland. It is trapped by the thyroid, but unlike iodine, it does not undergo organification and remains in the gland for a rela-

tively short duration. Therefore, imaging is done about 20–30 min after intravenous administration of the radiotracer. Approximately 5–10 mCi (185–370 MBq) are used. The thyroid-to-background activity ratio is not as high as that with radioiodine, so that ^{99m}Tc-pertechnetate is unsuitable for imaging to search for metastatic thyroid carcinoma, which usually functions poorly compared with normal thyroid tissue. Imaging of ectopic mediastinal thyroid tissue also may be suboptimal due to high blood and soft tissue background activity.

6.1.2.2 Iodine-123

Iodine-123 (^{123}I) has ideal characteristics for imaging the thyroid gland, with a short physical half-life of 13 h, absence of beta emissions, and high uptake in thyroid tissue relative to background [17]. However, it is less readily available and more expensive than ^{99m}Tc-pertechnetate. ^{123}I undergoes organic binding in the thyroid gland, and imaging is usually done 4–24 h after oral administration of 200–400 μCi (7.4–14.8 MBq) of radiotracer. Because of its superior biodistribution characteristics, ^{123}I is preferred over ^{99m}Tc-pertechnetate for imaging of poorly functioning and ectopic thyroid glands. ^{123}I also may be used for whole-body imaging in differentiated thyroid cancer. Approximately 2–4 mCi (74–148 MBq) of the radiotracer are used for this purpose.

6.1.2.3 Iodine-131

Iodine-131 (^{131}I) may be used for the measurement of thyroid uptake, which requires only very small amounts of radiotracer. It is no longer used for routine imaging of the thyroid gland but continues to be valuable for the detection of metastases and recurrences in differentiated thyroid cancer [3, 20, 21]. Following appropriate patient preparation to increase TSH levels, 2–4 mCi (74–148 MBq) of ^{131}I are administered orally and imaging is performed 48–96 h later. Radioiodine imaging has diagnostic as well as prognostic value. Iodine-avid tumors tend to be well-differentiated histological features and a favorable prognosis, whereas tumors that do not accumulate iodine are likely to be less differentiated and more aggressive [3, 22, 23].

Iodine-131 delivers a high radiation absorbed dose to the thyroid, with relative sparing of non-thyroid tissues. It is therefore ideal for the treatment of thyroid disease, and used extensively in the management of Graves' disease, toxic nodular goiter, and differentiated thyroid cancer.

6.1.2.4 Fluorine-^{18}F-Fluorodeoxyglucose (^{18}F-FDG)

Positron emission tomography (PET) with ^{18}F-FDG is used in evaluating a variety of neoplasms including differentiated thyroid cancer. In differentiated thyroid cancer, FDG may be used to identify metastases not visualized at radioiodine imaging, and to assess prognosis. Lesions that accumulate FDG tend to follow a more aggressive course than lesions that are not FDG-avid [10]. Whole-body FDG PET, therefore, is useful in evaluating high-risk thyroid cancer. Patient preparation is similar to that for radioiodine scintigraphy, since the uptake and diagnostic sensitivity of FDG are increased by TSH stimulation [11].

Focal uptake of FDG within the thyroid gland, an occasional finding at evaluation of non-thyroid cancers, may be related to a benign or malignant pathology [23]. In patients with thyroid nodules with indeterminate FNA, FDG PET/CT has a moderate ability to correctly discriminate malignant from benign lesions [24]. It may be a reliable option to reduce unnecessary diagnostic surgeries particularly if it is negative at the site of a solitary nodule. On the other hand, diffusely increased FDG uptake in the thyroid gland was found to be associated with chronic thyroiditis and thyroid dysfunction [25].

6.1.3 Major Thyroid Disorders

The most relevant thyroid conditions that commonly need imaging for diagnosis and management include nodular disease, inflammatory conditions, autoimmune disorders, and thyroid cancer:

6.1.3.1 Pathophysiology

Nodular Thyroid Disease

Thyroid nodules are common. The prevalence ranges from 4% to 10% in general adult and 0.2% to 1.5% in children [26] and is greater in countries affected by iodine deficiency. The incidence of thyroid nodules in apparently normal thyroid glands is greater than 50% in autopsy series. Studies using high frequency ultrasound in detecting nodules showed a varying prevalence of up to 68% [27, 28], higher in females compared to males and increasing with age [28].

Most thyroid nodules are benign, particularly in multinodular goiter. Malignancy in clinical thyroid nodules is reported to occur in 5–20% of nodules and is higher in males [29]. Mortality due to thyroid cancer is generally very low.

Types of Thyroid Nodules

Thyroid nodules represent wide spectrum of thyroid diseases. In a normal sized gland or a diffuse goiter, thyroid nodules may be solitary or multiple. In multinodular goiters, a nodule may become clinically dominant in terms of growth, dimensions, and functional characteristics. A clinicopathological classification of thyroid nodules subdivides nodules into: nonneoplastic nodules, true neoplastic nodules (benign or malignant), and micronodules.

Nonneoplastic Nodules (Pseudo-nodules)

These nodules may be seen in patients with thyroid hyperplasia, inflammatory or autoimmune thyroid diseases:

1. Glandular hyperplasia arising spontaneously or following previous partial thyroidectomy.
2. Rare forms of thyroid hemiagenesis which may present as hyperplasia of the existing thyroid tissue, mimicking a thyroid nodule.
3. Hashimoto's thyroiditis associated nodules, indicative of lymphocyte infiltration.
4. Nodules found during the initial phase of subacute thyroiditis, resulting from the inflammatory process.

Neoplastic Nodules

Based on scintigraphy thyroid nodules are classified into functioning (hot) nodules which are able to concentrate radioactive iodine or technetium-99m pertechnetate and non-functioning (cold) which show radiotracer uptake less than that in normal thyroid tissue. Hot nodules represent from 3% to 20% of thyroid nodules, according to the geographical origin of the patients as their incidence is higher in countries where iodine deficiency is still present. They are three to four times more frequent in females and tend to occur in those older than 40 years. In the great majority of cases, hot nodules are benign. Cold nodules account for more than 80% of all thyroid nodules. Three types of nodule are distinguished by ultrasonography: cystic, solid, and mixed (containing solid and cystic components). Cystic nodules (10–20% of all nodules) are almost always benign. Thyroid cancer is found in approximately 10% of cold nodules (solitary and multiple) that are solid or mixed at ultrasonography. More than 75% of malignant nodules are differentiated thyroid cancer of the follicular epithelium (papillary and follicular) with excellent prognosis. The other types of cancer are rare and include anaplastic or undifferentiated carcinoma (2–14% of all thyroid carcinomas), medullary thyroid carcinoma representing 5–10% of thyroid carcinomas and originating from the calcitonin-producing parafollicular C cells of the thyroid [30–32]. Lymphoma and metastases to thyroid are other uncommon malignancies.

Micronodules

Micronodules describe nodules of 1 cm or less in diameter. These nodules are discovered increasingly by the commonly used ultrasonography. In the absence of other suspicious clinical criteria, they only require to be followed by repeated thyroid ultrasonography.

Thyroiditis

Thyroiditis, a group of inflammatory thyroid diseases affecting the gland diffusely or focally, can be infectious, due to microorganisms, or noninfectious. Based on clinical, histopathologic, etio-

logical, and other factors, many classifications and terminologies for the conditions have been proposed. Simply it can be classified into acute, subacute, and chronic [32]. Figure 6.4 shows that classification which we modified to be more inclusive.

Acute Thyroiditis

Acute thyroiditis also called acute suppurative thyroiditis is a rare but serious form secondary to bacteria. Acute thyroiditis requires immediate parenteral antibiotic therapy before abscess formation begins.

Subacute Thyroiditis

Subacute thyroiditis or destructive thyroiditis is characterized by cell membrane breakdown and consequently release of excessive amounts of thyroid hormone into the circulation. The usual causes are autoimmune thyroid disease, viral infection, and amiodarone treatment. Less commonly, thyroiditis may be related to treatment with certain drugs such as interferon alpha, interleukin-2, lymphokine-activated killer (LAK) cells, and lithium. These therapeutic agents probably exacerbate existing autoimmune thyroid disease [3–6, 8–36].

Thyroiditis is typically painful and usually resolves spontaneously. Hyperthyroidism in the active phase is followed by transient hypothyroidism before restoration of the euthyroid state, usually in 6–12 months. Treatment usually consists of β-adrenergic blockers in the hyperthyroid phase and analgesics for pain. Protracted thyroiditis may however require glucocorticoids.

Viral subacute thyroiditis, also known as de Quervain's thyroiditis, usually occurs after an upper respiratory tract infection. The disorder tends to be seasonal and may occur in clusters, occasionally causing mini epidemics. It usually presents as a painful and tender goiter, associated with general malaise and possibly fever. Inflammation frequently begins in one lobe of the

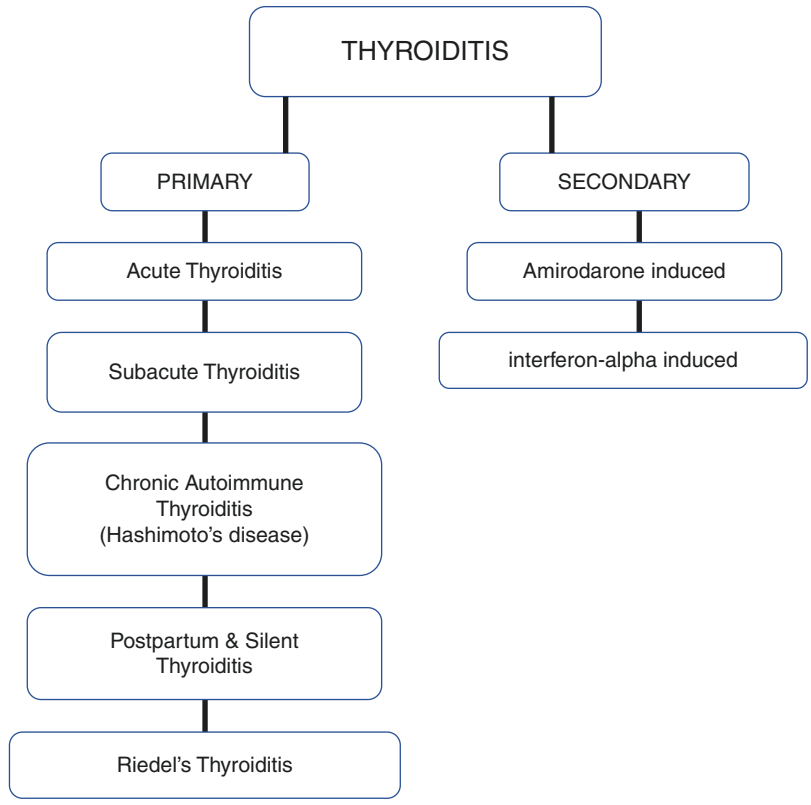

Fig. 6.4 Classification of thyroiditis

thyroid and gradually spreads to involve the entire gland. Permanent hypothyroidism is uncommon.

Postpartum Thyroiditis

Postpartum thyroiditis, also known as painless or subacute lymphocytic thyroiditis, is the principal thyroid disorder in postpartum women. It may be considered an accelerated form of autoimmune thyroid disease, attributed to suppression of immune-related disorders during pregnancy with a rebound after childbirth [37, 38].

For the same reason, Graves' disease also may occur in the postpartum period, though less frequently, and a strong association with insulin-dependent diabetes mellitus, an autoimmune condition, has been noted.

Postpartum thyroiditis, like other forms of destructive thyroiditis, is a self-limited, but tends to reoccur in subsequent pregnancies. Permanent hypothyroidism occurs in 20–25% of patients over a period of 5 years. Elevated thyroid peroxidase (anti-microsomal) antibodies during pregnancy are associated with a sharp increase in postpartum thyroiditis.

Amiodarone-Induced Thyroiditis

Amiodarone is an iodine-rich benzofuran derivative used to treat and prevent cardiac arrhythmias. It may precipitate a number of thyroid conditions including thyroiditis, which appears to be related to a cytotoxic effect [18, 19]. Thyroid hormone synthesis may increase or decrease. Other actions of amiodarone include blocking peripheral conversion of T_4 to T_3, binding of T_3 to its receptors, and thyroid release of T_3 and T_4. These effects may permit the use of amiodarone in very selected cases of hyperthyroidism [39].

Since amiodarone and its metabolite desethylamiodarone have long half-lives of up to 100 days, the thyroid-related effects can be protracted and occasionally may begin after stopping the drug. Amiodarone-induced thyroiditis generally requires treatment with a glucocorticoid. Permanent hypothyroidism is uncommon.

Interferon-Alpha Induced Thyroiditis

Interferon-alpha (IFNα) is an important drug therapy for several malignant and nonmalignant diseases, especially hepatitis C. Interferon induced thyroiditis is a major clinical problem for patients receiving interferon therapy. Studies have shown that up to 15% of patients with hepatitis C receiving IFNα develop clinical thyroid disease, and up to 40% were reported to develop thyroid antibodies. Interferon-alpha induced thyroiditis can be classified as autoimmune type and non-autoimmune type. Autoimmune interferon-alpha induced thyroiditis may be manifested by the development of thyroid antibodies with or without clinical disease. Clinical disease includes both autoimmune hypothyroidism (Hashimoto's thyroiditis) and autoimmune thyrotoxicosis (Graves' disease). Non-autoimmune thyroiditis can manifest as subacute (destructive thyroiditis) or as hypothyroidism with negative thyroid antibodies [40, 41].

Autoimmune Thyroiditis (Hashimoto's Disease)

See following section.

Autoimmune Thyroid Disease

Autoimmune thyroid disease is often observed together with other autoimmune diseases. The coexistence of two or more autoimmune diseases in the same individual is referred to as polyautoimmunity. The occurrence of polyautoimmunity has led to a hypothesis that the affected patients suffer from a generalized dysregulation of their immune system [42].

Autoimmune thyroid disease comprises two major entities, Hashimoto's disease (chronic autoimmune thyroiditis and variants) and Graves' disease. Variants of Hashimoto's disease include subacute thyroiditis, which occurs typically in the postpartum period, and atrophic thyroiditis. The predisposing factors of the disease are listed in Table 6.2 [43–46].

Hashimoto's Disease

Elevation of thyroid peroxidase antibodies is characteristic of Hashimoto's disease. Antithyroglobulin antibodies may also be elevated. Hormone synthe-

Table 6.2 Predisposing factors for autoimmune thyroid disease

Genetic predisposition Immune system dysregulation
Iodine excess
Cigarette smoking
Female gender
Psychological stress
Infection

sis is impaired with immune thyroid disease compensatory increase in TSH secretion, which stimulates thyroid function and growth. Eventually, many patients become hypothyroid. Both overt and subclinical hypothyroidism related to autoimmune disease are widely prevalent in iodine-sufficient regions [47].

Exacerbation of Hashimoto's disease, frequently occurring in the postpartum period, is a cause of subacute thyroiditis.

Graves' Disease

Graves' disease is associated with high levels of thyrotropin receptor autoantibodies(TRAB) that stimulate thyroid growth, and thyroid hormone synthesis and release [46, 48]. Most organ systems are affected by Graves' disease, the cardiovascular manifestations being the most apparent. Increased heart rate and contractility increases the cardiac output. These effects are related to a direct inotropic effect of T3, decreased systemic vascular resistance, increased preload related to a higher blood volume, and heightened sensitivity to sympathetic stimulation. Blood volume is increased by activation of the renin-angiotensin-aldosterone system caused by the reduction in systemic vascular resistance, and by increased erythropoietin activity. Overt cardiac failure may result from severe and prolonged hyperthyroidism, but is rarely seen today. Atrial fibrillation is not an uncommon complication, occurring in up to 15% of patients with hyperthyroidism [49, 50].

Autoimmune Interferon Induced Thyroiditis

The entire spectrum of autoimmune thyroid diseases (AITD) has been described in patients receiving IFNα: Graves' disease (GD), Hashimoto's thyroiditis (HT), and the presence of thyroid antibodies (TAb's) without clinical disease [40, 41].

Thyroid Cancer

In most areas of the world, the incidence of thyroid cancer of follicular origin is increasing. Currently the incidence is approximating 4/100,000 in males and 13.5/100,000 in females. Mortality is stable, at approximately 0.5/100,000 [51]. Based on the histologic classification nuclear medicine has a very important role in the management of thyroid cancer. Table 6.3 summarizes the classification of thyroid cancer. See Chap. 10.

6.1.3.2 Thyroid Scintigraphy

Nodular Disease

When thyroid nodule is discovered, the main problem is distinguishing between a benign and a malignant lesion. This problem has largely been solved by fine-needle biopsy which makes that distinction when performed by experienced cytologists. Nevertheless, nodules labeled as indeterminate by cytology remains a challenge [52]. Neck ultrasound plays a pivotal role in the diagnosis and several ultrasound stratification systems have been proposed in order to predict malignancy and help clinicians in therapeutic and follow-up decision. Despite new technologies in thyroid imaging, diagnostic surgery in 50–70% of patients with indeterminate cytology is still performed. In the last years, various image-guided procedures have been proposed as alternative and less invasive approaches to surgery for symptomatic thyroid nodules. These minimally invasive techniques (laser and radio-frequency ablation, high intensity focused ultrasound and percutaneous microwave ablation) result in nodule shrinkage and improvement of local symptoms, with a lower risk of complications and minor costs compared to surgery. Ultrasound-guided ablation therapy was introduced with promising results as a feasible treatment for low-risk papillary thyroid microcarcinoma or cervical lymph node metastases [52].

Accordingly, the role of thyroid scintigraphy is reserved to the assessment of the functional

Table 6.3 Types of thyroid cancer and main features

Type	Main features
Papillary carcinoma	Most common thyroid malignancy (85%). Derived from the follicular epithelium Has papillary growth pattern with psammoma bodies Has characteristic nuclear changes
Follicular variant papillary carcinoma	Follicular architecture with the characteristic papillary thyroid nuclear pattern
Papillary microcarcinoma	Added relatively recently Of less than 10 mm in size
Follicular carcinoma	Represents 10–20% of thyroid cancers Derived from follicular epithelium with evidence of capsular and/or vascular invasion but without nuclear changes characteristic of papillary thyroid cancer Have a slightly poorer prognosis than papillary cancer. Metastatic spread is hematogenous most commonly to the lung and bone
Oncocytic or Hurthle cell carcinoma	Hurthle cell can occur in any thyroid tumor More commonly associated with follicular carcinomas Prognosis is worse for comparative stage mainly due to poor radioiodine uptake
Poorly differentiated thyroid cancer	Formed of poorly differentiated cells Has a poor prognosis.
Anaplastic carcinoma	Formed of undifferentiated (anaplastic) cells Aggressive and has generally short clinical course and poor prognosis

activity of the nodules and when functional autonomy is suspected (Figs. 6.5, 6.6, and 6.7). Thyroid scintigraphy is performed then when serum TSH is suppressed or low in a patient with a single nodule and in all patients with multinodular goiter, regardless of the TSH result. Iodine-123 and ^{99m}Tc-pertechnetate are routinely used for imaging thyroid nodular disease. The acquisition of multiple projections is important as more than 30% of nodules can be missed with anterior views and only seen on the

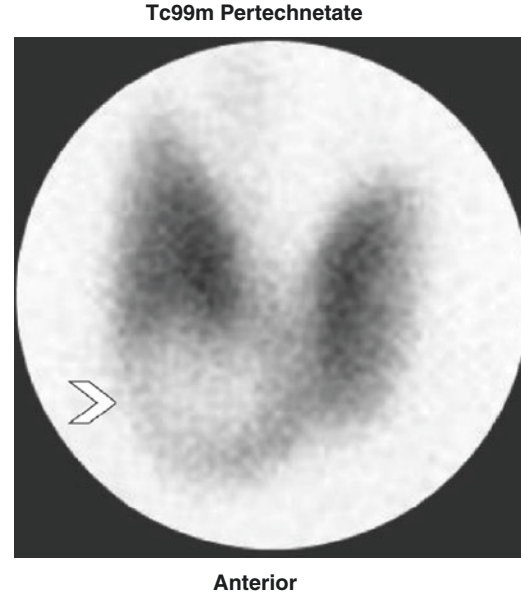

Fig. 6.5 Solitary cold nodule. ^{88m}Tc-pertechnetate thyroid scan anterior pinhole image showing a large solitary cold nodule (*arrow*)

oblique views [53]. ^{18}F-FDG PET has low specificity (63%) in the diagnosis of thyroid nodules but can help to select patients who need surgery when cytology is inconclusive in view of its high (100%) negative predictive value for thyroid cancer [52].

Whole-body ^{131}I and FDG PET have a role in the investigations and follow-up of thyroid cancer (see Chap. 10). On FDG PET scans, a normal thyroid gland demonstrates absent or low-grade FDG uptake. FDG PET may incidentally identify thyroid uptake. In general, a diffuse uptake by the thyroid gland is considered to be benign and very likely secondary to thyroiditis and/or hypothyroidism, while a focal uptake of the thyroid on FDG PET is defined as an incidentaloma, which is more clinically significant due to its high risk of malignancy ranging from 25% to 50% [54, 55].

Thyroiditis

Poor radioiodine/^{99m}Tc-pertechnetate uptake in the thyroid gland is the hallmark of subacute thyroiditis of any etiology (Fig. 6.8). Decreased tracer uptake is related to TSH suppression by excessive thyroid hormone released from

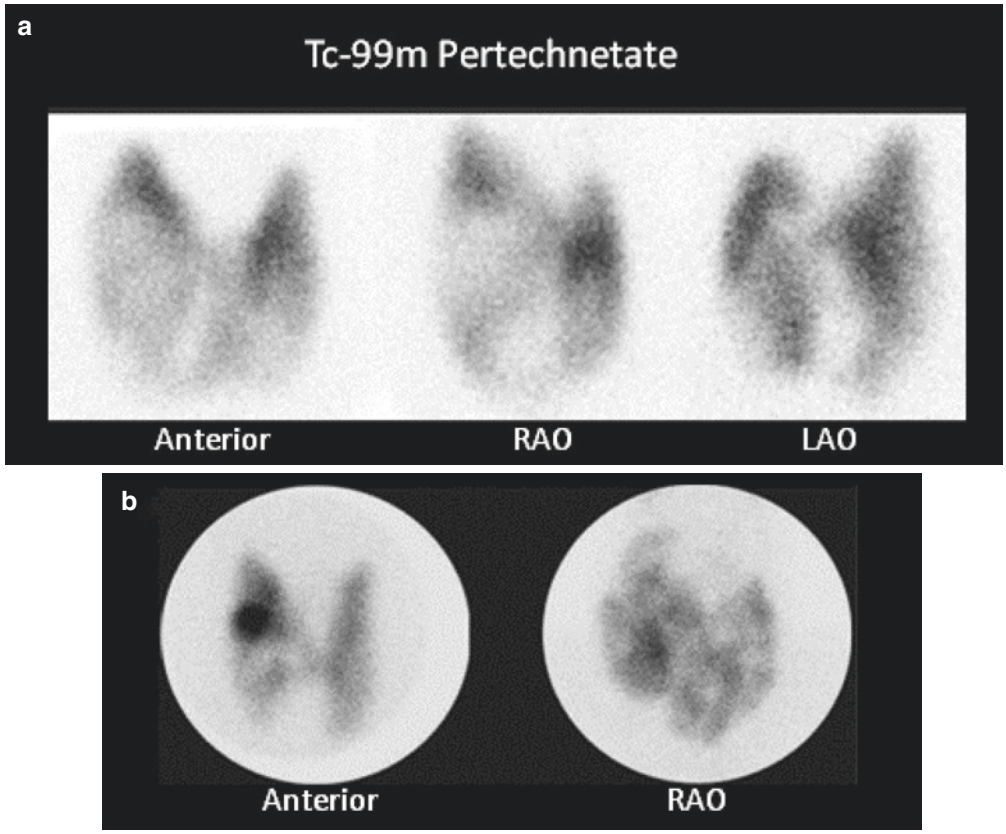

Fig. 6.6 Multinodular goiter as it appears on scintigraphy. (**a**) represents multiple cold nodules a while (**b**) shows mixture of cold and hot nodules

damaged follicles and to decreased hormone synthesis in the damaged gland. The thyroid uptake and scan normalize with resolution of thyroiditis.

Scintigraphy is frequently used in some thyrotoxic patients to differentiate autoimmune thyroiditis, with low uptake, from Graves' disease, with high uptake [48].

A thyroid uptake/scan may be worthwhile in amiodarone-related hyperthyroidism, which may be due to Jod-Basedow or thyroiditis. A low thyroid uptake is frequently found in patients treated with amiodarone and is nondiagnostic, while a normal or high uptake suggests that Jod-Basedow is likely. The thyroid uptake measurement also helps determine the feasibility of ^{131}I treatment in refractory cases.

Scintigraphy is nonspecific in Hashimoto's disease. The thyroid gland is usually symmetrically enlarged with uniform tracer distribution, and the 24-h radioactive iodine uptake is normal. In subacute thyroiditis resulting from exacerbation of Hashimoto's disease, tracer uptake is typically absent or very low.

Graves' Disease

Graves' disease typically shows uniformly increased tracer uptake in a diffusely enlarged thyroid gland (Fig. 6.9a), frequently with visualization of a pyramidal lobe and decreased background activity of various degrees based on the severity of the condition (Fig. 6.9b). However, atypical appearances, particularly in Graves' disease superimposed on nodular goiter, are

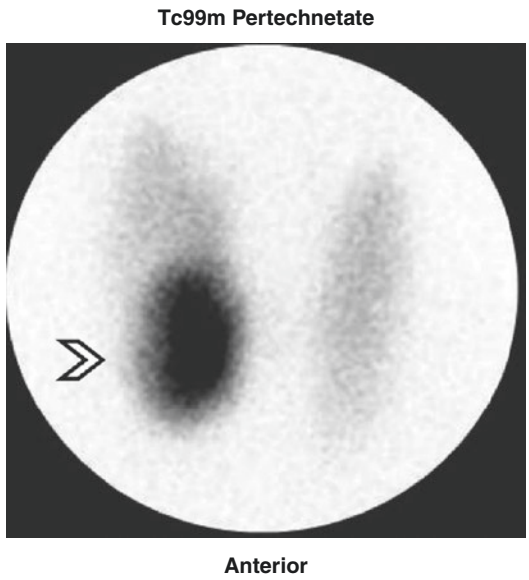

Fig. 6.7 Solitary hot nodule. A study showing a toxic nodule in the right lower lobe (*arrow*) with suppression of the remainder of the gland

occasionally encountered. If needed, TRAB measurement may assist in confirming the diagnosis. The 24-h radioactive iodine uptake is elevated and, typically, much higher than in toxic nodular goiter [49, 56].

6.1.4 Thyroid Dysfunction and Pregnancy

Results from observational studies have indicated that even mild to moderate iodine deficiency in pregnancy might negatively affect child neurodevelopment [57–59]. Low maternal free T_4 (FT4) has been suggested to be associated with poor child neurodevelopment. A recent meta-analysis of individual participants data from 9036 mother–child pairs from three prospective population-based birth cohorts from Spain, Netherlands, and the United Kingdom indicates that low maternal FT4 was consistently associated with a lower child IQ [60].

Hyperthyroidism in pregnancy is generally caused by Gestational Transient Thyrotoxicosis (GTT) or Graves' disease. Management of Graves' disease remains a challenge, with thionamide treatment as the best option. Patients should be monitored closely because undertreatment, with persistently high maternal TRAB, increases the risk of fetal hyperthyroidism, while overtreatment may cause fetal hypothyroidism. Gestational hypothyroidism is usually related to autoimmune thyroid disease, and less frequently to iodine deficiency. The latter may be associated with fetal hypothyroidism as well.

6.1.5 Summary

Synthesis and secretion of thyroid hormone are regulated mainly by thyroid releasing hormone and thyroid-stimulating hormones. Thyroid-stimulating hormone promotes iodide transport and the synthesis and release of thyroid hormones and thyroglobulin. Excessive amounts of iodine may cause hypothyroidism or hyperthyroidism. Endemic goiter is the result of iodine deficiency, with decrease in hormone production and compensatory increase in TSH secretion. Thyroid nodules represent a wide spectrum of thyroid diseases. Thyroid nodules may be solitary or multiple. A clinicopathological classification of thyroid nodules subdivides nodules into nonneoplastic nodules, true neoplastic nodules (benign or malignant), and micronodules. Autoimmune thyroid disorders, including Hashimoto's disease and Graves' disease, are related primarily to genetic susceptibility, with contributions from environmental factors including chronic iodine excess. Subacute thyroiditis is usually caused by exacerbation of autoimmune disease, viral infection, and amiodarone or interferon-alpha therapy. Iodine deficiency in pregnancy might negatively affect child neurodevelopment.

6.2 Parathyroid Gland

6.2.1 Anatomical and Physiological Considerations

Normal parathyroid glands are derived from the pharyngeal pouches, the upper glands from the endoderm of the fourth pouch, and the lower

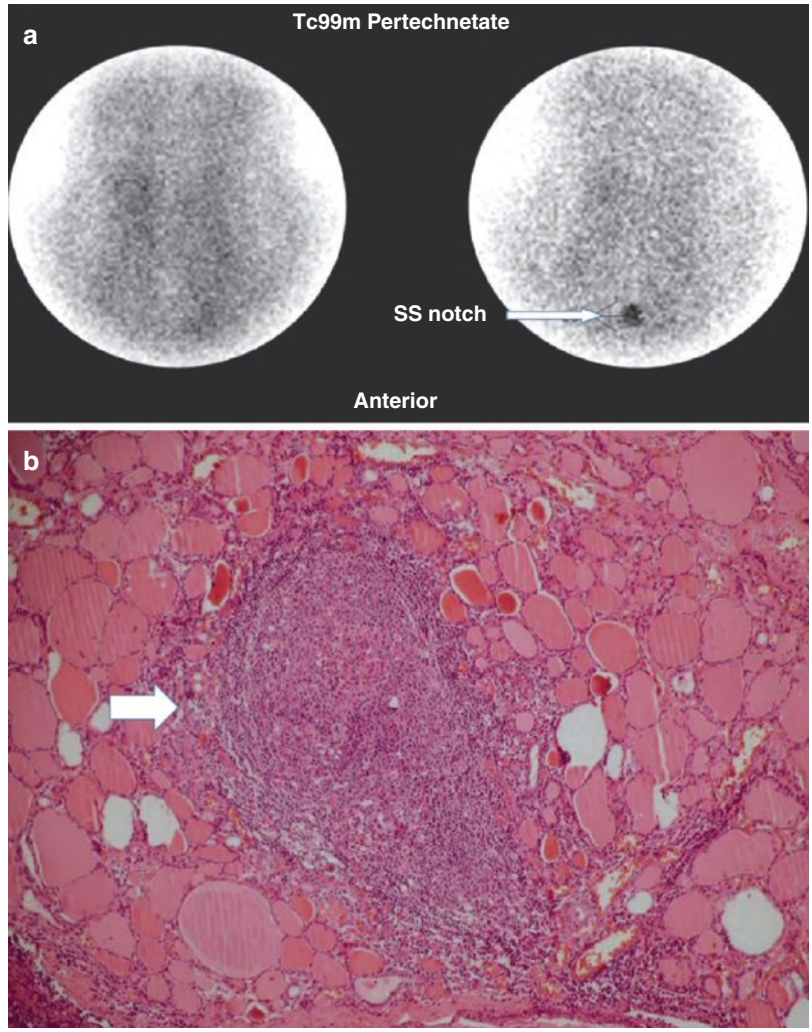

Fig. 6.8 Thyroiditis (**a**, **b**). (**a**) ^{99m}Tc-pertechnetate thyroid scan in an 8-year-old girl with a recent history of upper respiratory infection. The scan shows poor uptake by the thyroid gland with poor delineation of its outlines. The thyroid uptake was 0%. SS notch: suprasternal notch. (**b**) Microscopic illustration of thyroiditis with a focus of inflammatory cells (*arrow*) surrounded by thyroid follicles. (Courtesy of Professor Magda El-Monayeri with thanks)

glands from the third pouch. The parathyroid glands are typically located on the posterior aspect of the thyroid gland (Fig. 6.1). Occasionally one or more glands may be embedded in the thyroid. The normal position of the superior parathyroids is at the cricothyroid junction, above the anatomical demarcation of the inferior thyroid artery and the recurrent laryngeal nerve [61]. The inferior parathyroids are more widely distributed mostly anterolateral or posterolateral to the lower thyroid gland [62]. The accessory glands that can be variously located in humans, from the cricoid cartilage down into the mediastinum [63, 64], are derived from the numerous dorsal and ventral wings of the pouches. Normally, human beings have four glands, but more or fewer than this number are found in some individuals [49]. Among healthy adults, 80–97% have four parathyroids; approximately 5% have fewer than four glands, and 3–13% have supernumerary glands [62]. Location and anatomy of parathyroid glands are essential for surgical planning and for carrying out parathyroidectomies since any unidentified gland, either supernumerary or in ectopic location, can result in unsuccessful treatment and possible reoperation. Recent large meta-analysis study showed that 81.4% of patients have four glands with 15.9% of the glands are ectopic (11.6% in the neck and 4.3% in the mediastinum). Additionally, 51.7% of the neck ectopic

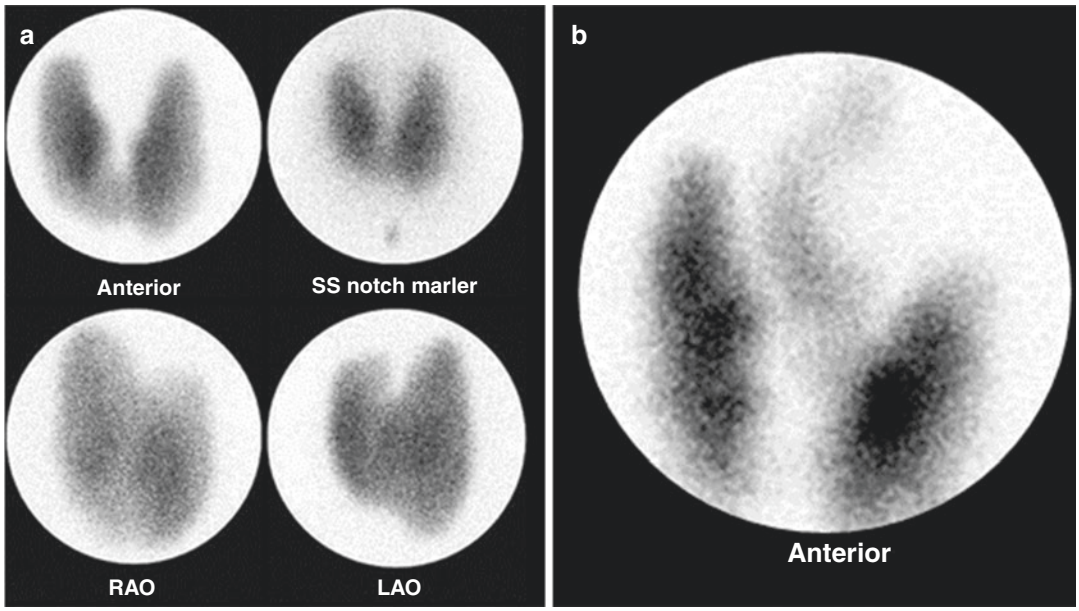

Fig. 6.9 (**a**) Graves' disease. ^{99m}Tc-thyroid scan illustrating the pattern of Graves' disease. There is uniform increased radionuclide distribution with low background activity. (**b**) Anterior view of tc99m pertechnetate illustrating Grave's disease with visualized pyramidal lobe and decreased background uptake

glands are located in retroesophageal/paraesophageal space or in the thyroid gland [63].

The normal glands usually measure 4–6 mm in length, 2–4 mm in width, and 0.5–2 mm in thickness. The glands are usually ovoid or bean shaped but may be elongated, flattened into a leaf-like structure, or multilobulated. The weight of the glands is usually 30 mg each, with the largest normal gland not exceeding 70 mg. The total weight of the glands is less than 210 mg, and the total parenchymal cell weight is less than 145 mg [64]. In normal glands, parenchymal cells are predominantly chief cells which contain cytoplasmic fat droplets. Oxyphilic and transitional oxyphilic cells are sparsely present in children and young adults and increase to 4–5% of the parenchymal cells in old age. These cells tend to form nodules if they increase in number and have a very small amount of fat or no fat at all in their cytoplasm. Ultrastructurally, oxyphil cells are characterized by the presence of closely packed mitochondria, while chief cells contain moderate to high mitochondrial content. Water-clear cells are vacuolated with distended organelles. Each of the three cell types may contain varying amounts of lipid droplets and residual bodies [65]. Table 6.4 summarizes the types of parathyroid cells and their function.

Table 6.4 Cells of the parathyroid glands and their functions

Cell type	Major ultrastructural feature	Function
Chief cell	Slightly eosinophilic cytoplasm, few mitochondria	The active endocrine cell, producing the parathyroid hormone
Oxyphil cell	Rich eosinophilic cytoplasm, tightly packed mitochondria	May be able to produce parathyroid hormone
Transitional oxyphil cell	Less eosinophilic cytoplasm	Variant of oxyphil cell
Clear cell	Foamy and water-clear cytoplasm	Unknown, fundamentally inactive

Parathyroid hormone has four principle actions: (a) to increase calcium absorption from the gastrointestinal tract; (b) to stimulate osteoclastic activity, resulting in resorption of calcium

and phosphate from bone; (c) to inhibit phosphate reabsorption by the proximal renal tubules; and (d) to enhance renal tubular calcium reabsorption. Parathyroid hormone secretion is controlled mainly by the extracellular calcium concentration. The parathyroid cell surface is thought to be equipped with a cation-sensitive receptor mechanism through which ambient calcium regulates the cytosolic calcium ($Ca^{2+}i$) concentration and parathyroid hormone secretion. Activation of this receptor causes also activation of protein kinase C. 1,25-Dihydroxycholecalciferol reduces the secretion of parathyroid hormone independent of any changes in calcium concentration. Parathyroid hormone is metabolized in Kupffer's cells of the liver.

In patients with hyperparathyroidism, pathological parathyroid cells show defective sensing of ambient calcium. The cellular basis of this abnormality is unknown, although increased protein kinase C activity within abnormal parathyroid cells may be the mechanism. Pathological parathyroid glands also have an increased parenchymal cell content, although the extent of hypercalcemia appears more closely related to the defective secretory regulation than to increased parenchymal cell mass [66].

6.2.2 Hyperparathyroidism

Hyperparathyroidism has been diagnosed with increasing frequency in recent years due to awareness of the disease and to the laboratory advancement that allowed for routine chemistry screening. The condition is characterized by excess secretion of parathyroid hormone. The resulting biochemical changes, including increased levels of serum calcium and increased urinary excretion of calcium, may result in calcium wastage, nephrocalcinosis, urolithiasis, bone disease, and neuropsychiatric disturbances. Hyperparathyroidism may occur as a primary, secondary, or tertiary disease. It can also occur as eutopic and ectopic disease. In addition, it may have a familial origin, as in multiple endocrine neoplasia (MEN).

6.2.2.1 Primary Hyperparathyroidism

Primary hyperparathyroidism is a common endocrine disorder of calcium metabolism characterized by hypercalcemia and elevated or inappropriately normal concentrations of parathyroid hormone. Almost always, it is due to a benign overgrowth of parathyroid tissue either as a single gland (80% of cases) or as a multiple gland disorder (15–20% of cases) [67]. It is the most common cause of hypercalcemia in postmenopausal women [68]. Primary hyperparathyroidism occurs due to neoplastic or hyperplastic parathyroid glands or when nonparathyroid tumors such as bronchogenic or renal cell carcinomas secrete ectopically parathyroid hormone or a biologically similar product. The incidence of this disorder in the United States is estimated to be 66 per 100,000 person among women and 25 per 100,000 among men per year [69, 70]. The condition is more prevalent in females than males by a ratio of 3 to 1. More than 80% of patients with primary hyperparathyroidism have a solitary adenoma. Hyperplasia—predominantly of chief cells—occurs in less than 20% of patients. Parathyroid carcinoma is the cause in less than 1% of patients, and very rarely the condition is due to ectopic secretion of parathyroid hormone [64, 65].

Primary hyperparathyroidism occurs as part of MEN. MEN is a hereditary syndrome that involves hyperfunctioning of two or more endocrine organs. Primary hyperparathyroidism, pancreatic endocrine tumors, and anterior pituitary gland neoplasms characterize type 1 MEN. MEN 2A is defined by medullary thyroid carcinoma, pheochromocytoma (about 50%), and hyperparathyroidism caused by parathyroid gland hyperplasia (about 20%). MEN 2B is defined by medullary thyroid tumor and pheochromocytoma. Both MEN 1 and MEN 2 are inherited autosomal dominant cancer syndromes. The gene responsible for MEN 1 is a tumor suppressor gene located on chromosome 11 [71, 72].

Primary hyperparathyroidism is also associated with thyroid pathology in 15–70% of patients [73, 74]. This includes thyroid carcinoma which has been reported in the range of

1.7–6.2% of patients with primary hyperparathyroidism [73–75].

6.2.2.2 Secondary Hyperparathyroidism

Secondary hyperparathyroidism occurs when there is a condition causing chronic hypocalcemia such as chronic renal failure, malabsorption syndromes, dietary rickets, and ingestion of drugs such as phenytoin, phenobarbital, and laxatives, which decrease intestinal absorption of calcium. Secondary hyperparathyroidism is simply a compensatory hyperplasia in response to hypocalcemia. In this condition, reduced renal production of 1,25-dihydroxyvitamin D_3 (active metabolite of vitamin D) leads to decreased intestinal absorption of calcium, resulting in hypocalcemia. Tubular failure to excrete phosphate results in hyperphosphatemia. Hypocalcemia along with hyperphosphatemia is compensated for by hyperplasia of the parathyroids to overproduce PTH. Secondary hyperparathyroidism develops in chronic kidney disease, which is due to a combination of vitamin D deficiency, hypocalcemia, and hyperphosphatemia, and it exists in nearly all patients at the time of dialysis initiation [76].

6.2.2.3 Tertiary Hyperparathyroidism

Tertiary hyperparathyroidism describes the condition of patients who develop hypercalcemia following long-standing secondary hyperparathyroidism due to the development of autonomous parathyroid hyperplasia, which may not regress after correction of the underlying condition, as with renal transplantation.

6.2.2.4 Eutopic Parathyroid Disease

Parathyroid disease with typical location of glands (eutopic) represents 80–90% of all cases. There is a relatively fixed location for the superior parathyroids and are found close to the dorsal aspect of the upper thyroid [61, 62]. On the other hand, inferior parathyroids have a more widespread distribution, which is closely related to the migration of the thymus. Inferior parathyroids are mostly located inferior, posterior, or lateral to the lower thyroid. They may be very close to the thyroid and may be covered by or attached to the thyroid capsule and are sometimes adjacent to or surrounded by remnant thymic tissue. Interestingly, the parathyroid glands demonstrate a remarkably constant symmetry, which is helpful in the surgical exploration of eutopic disease [62].

6.2.2.5 Ectopic Parathyroid Disease

Superior parathyroid adenoma may have an abnormal supero-posterior mediastinal position, such as a retropharyngeal, retroesophageal, or paraesophageal site or the tracheoesophageal groove. The frequency of ectopia (up to 39%) is similar for the right and left superior parathyroids [77]. Intrathyroid superior parathyroid adenomas are rare.

The more common ectopic inferior parathyroids are a well-established entity responsible for 10–13% of all cases of hyperparathyroidism [77]. Ectopic tissue can occur from the angle of the mandible to the mediastinum according to the developmental and migratory aberrations. These sites include the mediastinum, thymus, aortopulmonary window, carotid bifurcation and rarely thyroid, carotid sheath, vagus nerve, retroesophageal region, thyrothymic ligament, and pericardium [77, 78].

6.2.3 Parathyroid Adenoma

Parathyroid adenoma is a benign tumor that is usually solitary, although multiple adenomas are found in a low percentage. The tumor in general is more common in women and varies in weight from less than 100 mg to more than 100 g. The most commonly found adenomas, however, weigh 300 mg to 1 g. The size was found to correlate to the degree of hypercalcemia.

Microscopically, the vast majority of typical adenomas are formed predominantly of chief cells, although a mixture of oxyphil cells and transitional oxyphil cells is also common. Adenomas formed of water-clear cells are very rare. A rim of parathyroid tissue is usually present outside the capsule of the adenoma and can serve to distinguish it from parathyroid

Table 6.5 Variants of parathyroid adenoma [79–88]

Type	Major features	Imaging
Solitary adenoma	Found in 80–85% of patients with primary hyperparathyroidism	^{99m}Tc-MIBI with high sensitivity
	Composed of chief cells or mixture of chief, oxyphil, or transitional oxyphil cells	
Double/ multiple	Occurs in up to 12% of cases of primary hyperparathyroidism	Detection with any imaging modality is not reliable
	Bilateral in 55–88% of cases	^{99m}Tc-MIBI has a sensitivity of less than 37%
	More prominent symptoms and higher parathyroid hormone and alkaline phosphatase levels than with a solitary adenoma or hyperplasia	
Cystic adenoma	Central necrosis or cystic degeneration of adenomas	May not be visualized on ^{99m}Tc-MIBI studies
	Accounts for less than 9% of all parathyroid adenomas	
	Frequently associated with hyperparathyroidism	
Lipoadenoma	Composed of hyperfunctioning parathyroid tissue and fatty stroma	Target-to-background ratio may be low due to the high adipose content
Oncocytic adenoma	Rare subtype formed of 80–100% oxyphil cells	^{99m}Tc-MIBI with high sensitivity

carcinoma. The chief cells in adenomas are usually enlarged, and their nuclei are larger and more variable in size than in normal chief cells. Nuclear pleomorphism may be prominent; this is not considered a sign of malignancy but a criterion for discriminating adenoma from hyperplasia, which lacks this feature. The following variants (Table 6.5) of parathyroid adenoma may be recognized.

6.2.3.1 Solitary Adenoma

Solitary adenoma is found in 80–85% of patients with primary hyperparathyroidism [9]. There is no significant predominance in location among the four parathyroids with each responsible for approximately 25% of all solitary adenomas [77]. The remaining tumor-free parathyroid glands associated with single adenomas usually have lower weight and parenchymal cell mass than the average normal glands and show signs of secretory inactivity on electron microscopy.

6.2.3.2 Double or Multiple Adenomas

Double or multiple adenomas occur in up to 12% of cases of primary hyperparathyroidism [79, 80]. These patients have more prominent symptoms and usually have higher parathyroid hormone and alkaline phosphatase levels than those with a solitary parathyroid adenoma or hyperplasia. Preoperative detection of double or multiple adenomas with any imaging modality is not reliable [81, 82].

6.2.3.3 Cystic Adenoma

Cystic adenomas are thought to represent central necrosis or cystic degeneration of adenomas [85]. Contrary to the asymptomatic true parathyroid cysts which are due to embryologic vestiges of the third and fourth pharyngeal pouches or enlargement of microcysts within the parathyroid as a manifestation of colloid retention [86], cystic adenomas are frequently associated with hyperparathyroidism.

6.2.3.4 Lipoadenoma

Parathyroid lipoadenoma, composed of hyperfunctioning parathyroid tissue and fatty stroma, is a rare entity that occurs in patients beyond the fourth decade of life.

6.2.3.5 Oncocytic Adenoma

Oncocytic adenoma is a rare subtype and has been reported to be associated with hyperparathyroidism. It is found in the sixth or seventh decades and like the typical adenomas is more common in women [88].

6.2.4 Parathyroid Hyperplasia

Parathyroid hyperplasia affects the glands to varying degrees, and commonly one or two glands are of normal size even though microscopic signs of endocrine hyperfunction are present, at least focally, in all glands. Chief cell hyperplasia is the most common and is composed of chief cells or a mixture of chief cells and to a lesser extent oxyphil cells. The cells are arranged diffusely, in nodules, or in a mixture of both patterns. Water-clear cell hyperplasia is rare and is characterized by substantial enlargement of most parathyroid glands. The large water-clear cells are usually arranged in a diffuse pattern [89].

In primary hyperparathyroidism, hyperplasia affects the glands asymmetrically. In secondary hyperparathyroidism, the hyperplastic glands are more uniformly enlarged than with primary chief cell hyperplasia, with two histological types (Table 6.6). In the tertiary form, the glands are more often markedly and asymmetrically enlarged.

Pathologically, it is difficult to differentiate primary chief cell hyperplasia of only one gland from adenoma. Both contain large numbers of active chief cells with cells characterized by aggregated arrays of rough endoplasmic reticulum and a large, complex Golgi apparatus with numerous vacuoles and vesicles. Secretory granules are frequently present in these cells. These changes indicate that most of these cells are in the more active phases of parathyroid hormone synthesis and secretion [90]. Molecular biology techniques used on pathological parathyroid tissue have shown that cell proliferation is monoclonal in many sporadic adenomas and in the largest glands of multiple endocrine neoplasia type I. This monoclonality has not been found in the smaller parathyroid glands of multiple endocrine neoplasia or in sporadic hyperplasia. Additionally, rearrangement of parathyroid hormone gene in chromosome 11 was observed in sporadic adenomas.

Table 6.6 Classification of parathyroid hyperplasia

Type	Major pathological features
Primary hyperplasia	Uniform chief cells with some oxyphil and transitional oxyphil cells
Secondary hyperplasia	
Diffuse(classic) type	Cords, sheets, or follicular arrangement of cells replacing the stromal fat cells. Oxyphil cells are more frequent in this type. This type is indistinguishable from the primary type
Adenomatous-nodular type	Cells are grouped in large islands or nodules. Necrosis is seen more frequently than in diffuse type

6.2.5 Parathyroid Carcinoma

Parathyroid carcinoma is a rare cause of hyperparathyroidism which can arise in any parathyroid gland, including ectopic and mediastinal, although the usual site of involvement is the normally located parathyroids. The tumor is found predominantly in patients between the ages of 30 and 60 years, with no sex preference, and is usually functioning. The tumors tend to be larger than adenomas and appear as lobulated, firm, and uncapsulated masses that often adhere to the surrounding soft tissue structures. The involved glands usually weigh more than 1 g and the diagnosis is restricted histologically to the lesions displaying infiltrative growth into vessel or capsule, since pleomorphism can be seen in many adenomas.

6.2.6 Hyperfunctioning Parathyroid Transplant

Autotransplantation of parathyroid tissue is performed in cases of recurrent, persistent type 1 MEN and symptomatic secondary hyperparathyroidism in association with total parathyroidectomy. After total parathyroidectomy, the most normal glands, usually one or two, are used for the graft. They are diced into small fragments with each fragment placed in an individual bed beneath a muscle sheath and between muscle fibers [91]. A graft site in the forearm is preferred for accessibility. The graft may be functional in 8–9 days after surgery [80]. After autotransplan-

tation, recurrent hyperparathyroidism occurs in approximately 14% of cases [92]. A hyperfunctioning graft in the forearm is easily demonstrated with Doppler US or ^{99m}Tc-sestamibi scintigraphy [92].

6.2.7 Consequences of Hyperparathyroidism

Excess secretion of parathyroid hormone promotes bone resorption and consequently leads to hypercalcemia and hypophosphatemia. The clinical presentation and complications of hyperparathyroidism depend on the rapidity of development and the degree of hypercalcemia. They can be grouped into genitourinary, gastrointestinal and musculoskeletal, neuropsychiatric, and others (Table 6.7).

The five disease-specific symptoms are muscle weakness, polydipsia, dry skin and itching, memory loss, and anxiety. Overall the symptoms, particularly the disease-specific ones, show significant decline after successful parathyroidectomy [93].

Table 6.7 Consequences of hyperparathyroidism

Type of abnormality	Presentation
Genitourinary	Nephrolithiasis
	Nephrocalcinosis
	Renal insufficiency
	Polyuria
	Nocturia
	Decreased urine concentrating ability
Gastrointestinal	Nausea
	Vomiting
	Constipation
	Increased thirst
	Loss of appetite
	Abdominal pain
	Peptic ulcers
	Heartburn (hypercalcemia causes increased gastric acidity)
	Pancreatitis
Musculoskeletal	Myopathy
	Muscle weakness
	Osteoporosis
	Osteomalacia
	Bone and joint pains
	Renal osteodystrophy
	Pseudogout
Neuropsychiatric	Memory loss
	Anxiety
	Sleepiness
	Confusion
	Lassitude, coma
	Depression
	Impaired thinking
	Psychosis
Others	Fatigue
	Hypertension
	Pruritis
	Metastatic calcification including cardiocalcinosis
	Band keratopathy (present in the medial and lateral aspects of the cornea)

6.2.8 Preoperative Parathyroid Localization

Surgery is the major and only current curative modality in treating primary hyperparathyroidism. Identifying the glands can be difficult, however, particularly with removal of multiple glands and with reoperation [94]. Although the success rate is high in experienced hands, up to 25% of the initial explorations fail because the abnormal glands cannot be located. Prolonged exploration was also found to result in a high incidence of recurrent laryngeal nerve damage [94]. Surgical re-exploration with violated anatomy is even more difficult and hazardous and can often be unrewarding.

Preoperative localization of parathyroid lesions is thus desirable to reduce the incidence of missed lesions and to help avoid prolonged neck exploration. Since surgeons' experience with neck exploration is decreasing due to the reduced incidence of thyroid surgery with the expanding use of iodine-131 for therapy of hyperthyroidism, preoperative localization of parathyroid lesions is even more important than before.

In recent years, minimal access parathyroid surgery (small incisions with gamma probe or endoscopic assistance) is increasingly becoming the operation of choice for single parathyroid adenomas [95]. Compared with bilateral neck exploration, it has a shorter hospital stay, less morbidity, and better cosmetic result [95]. The development of this minimally invasive surgical techniques has placed an even greater emphasis on preoperative localization [96].

The forms that preoperative localization can take include computed tomography (CT), ultrasound, magnetic resonance imaging (MRI), arteriography, selective venous sampling, ^{99m}Tc-sestamibi (MIBI) scintigraphy, ^{18}F-fluorodeoxyglucose positron emission tomography (FDG PET), and ^{11}C-methionine PET. The morphological imaging modalities, such as CT, ultrasound, and MRI, have the disadvantage that they cannot distinguish functional parathyroid tissue from other types of tissue. However, they provide excellent image resolution and contrast. Overall their accuracy is inadequate and varies.

6.2.9 Scintigraphic Localization

Scintigraphy using ^{99m}Tc-sestamibi (MIBI) is currently the preferred nuclear medicine method for parathyroid imaging. It is the most sensitive and cost-effective modality for preoperative localization of hyperfunctioning parathyroid tissue. If a single parathyroid adenoma is detected, a unilateral scan-directed neck exploration can be performed. Due to a wide variation in scintigraphic techniques [97], the reported sensitivities of MIBI scan range from 80% to 100%. The mechanism of uptake of this radiopharmaceutical by abnormal parathyroid cells is not fully understood although the mitochondria have been implicated in its uptake [98]. P-glycoprotein, a membrane transport protein encoded for by the multidrug resistance (MDR) gene, may also be additionally responsible for uptake, since it transports other products with structural similarity to MIBI [99]. The uptake and retention of MIBI by the abnormal neoplastic and hyperplastic lesions are probably due to the alterations in the biology of the abnormal parathyroid cells, as noted earlier, and mitochondria are probably the site of retention. The size of the lesions is also an important factor in their visualization but cannot alone explain the uptake and retention. The size and the cellularity of the abnormal gland are also factors in the visualization and correlate with its MIBI uptake (Fig. 6.10) [100, 101]. Additionally, the ectopic disease (Fig. 6.11) may affect the degree of visualization and SPECT with or without CT is better to be used.

Parathyroid lesions detected by ^{201}Tl scintigraphy have been shown to have significantly higher numbers of mitochondria-rich oxyphil cells compared with nonvisualized lesions, indicating further that the uptake depends in part on the metabolic activity of the lesion [102]. Our group found that the amount of mitochondria (Fig. 6.11) in adenoma cells correlates with the degree of uptake [103]. Significant P-glycoprotein or multidrug resistance-related protein expression was reported to limit the sensitivity of MIBI imaging in localizing parathyroid adenomas [98].

The protocol for MIBI parathyroid scintigraphy varies regarding timing of acquisition, SPECT and SPECT/CT. However, the study principle is to acquire early and delayed (Figs. 6.12 and 6.13). The variable behavior of abnormal parathyroid glands is due to the varying ultrastructure of the cells, the various combinations of cell types, and their biological activity. ^{123}I or pertechnetate thyroid imaging for comparison or subtraction is only occasionally needed on an individual basis (e.g., presence of thyroid nodule). If the presence of thyroid pathology is known or suspected clinically, one starts with a thyroid scan to define the morphology and localize the thyroid by injecting 1 mCi ^{99m}Tc-pertechnetate i.v., and the neck is imaged 15 min later.

Tetrofosmin has been also used in a 2-day protocol using ^{99m}Tc-pertechnetate imaging of thyroid and single acquisition of ^{99m}Tc-Myoview next day. Comparing the activity of both scans

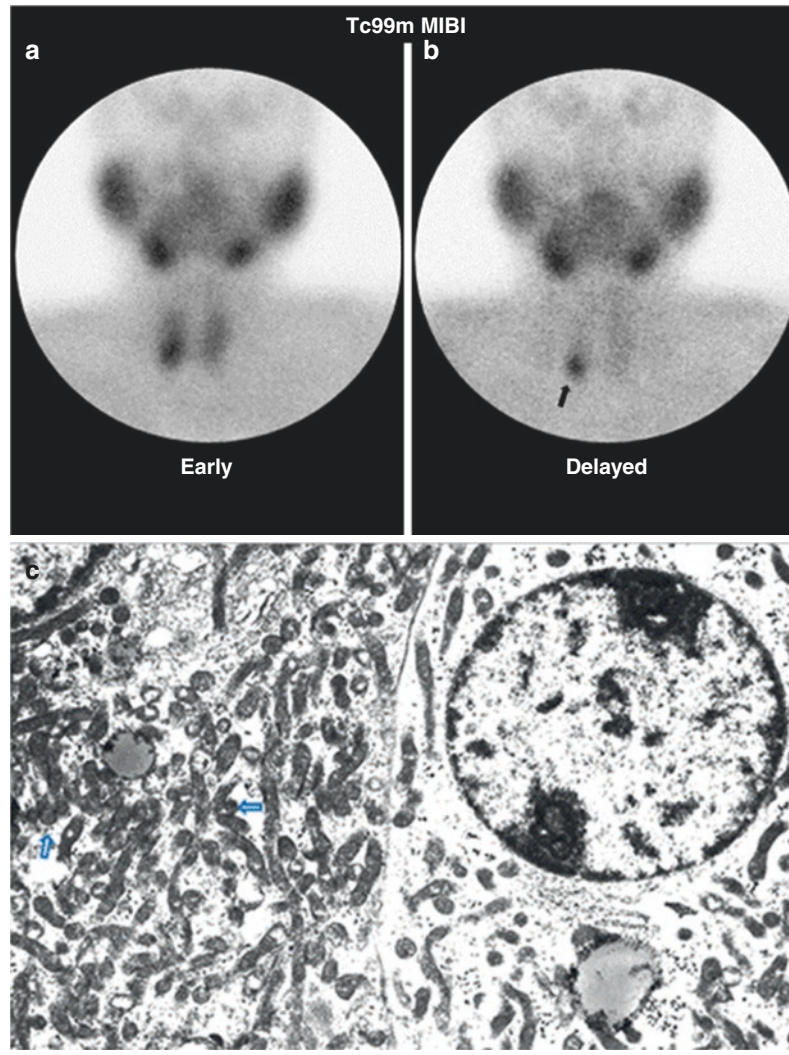

Fig. 6.10 Tc99m sestamibi study for a patient with biochemically proven hyperparathyroidism. Early images (**a**) shows a focus of increased uptake in the region of the right lower pole of the thyroid gland which, in the delayed image (**b**), retains the activity (arrow) with clearance of thyroid uptake consistent with adenoma. Surgery was performed and the lesion was pathologically proven to be adenoma. Sample was sent for electron microscopic study. Electron microscopic photograph (**c**) of this parathyroid adenoma illustrates cells packed with mitochondria (arrows)

obtained 15 min post injection facilitates detecting focal activity of parathyroid adenomas and hyperplastic glands with high accuracy [104].

It was reported that parathyroid scan interpretation by a nuclear medicine physician along with an endocrine surgeon resulted in improved accuracy of gland localization and lateralization compared to a nuclear medicine physician reading alone. This improvement may be due to increased awareness of clinical data and head and neck anatomy [105].

SPECT/CT has proven to be most accurate in localizing parathyroid glands (Fig. 6.14) and is currently the recommended procedure. It has proven to be a useful tool for preoperative assessment, not only for ectopic glands but also for patients with previous neck surgery. It also increases reporting confidence for physicians [106, 107]. It has been reported to be 94% accurate in detecting parathyroid adenoma and 92% in accurate localization [108].

PET has been also investigated for localizing parathyroid glands. Initial studies using FDG showed conflicting results in imaging the parathyroid glands in primary hyperparathyroidism. ^{11}C-methionine PET was suggested to be more promising than FDG in parathyroid localization [109]. In a large recent study of 171 patients,

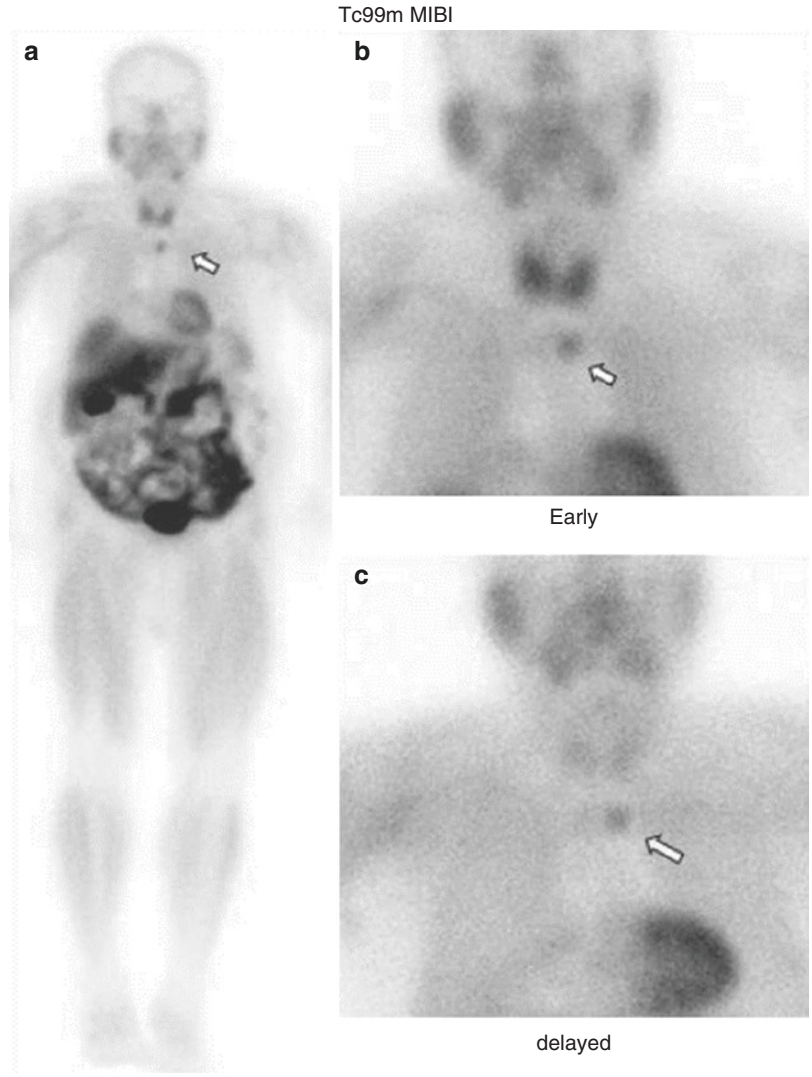

Fig. 6.11 Ectopic parathyroid adenoma (*arrow*) seen on Tc99m MIBI study. Early whole-body (**a**) and spot images (**b**, **c**) with retained activity on delayed spot image

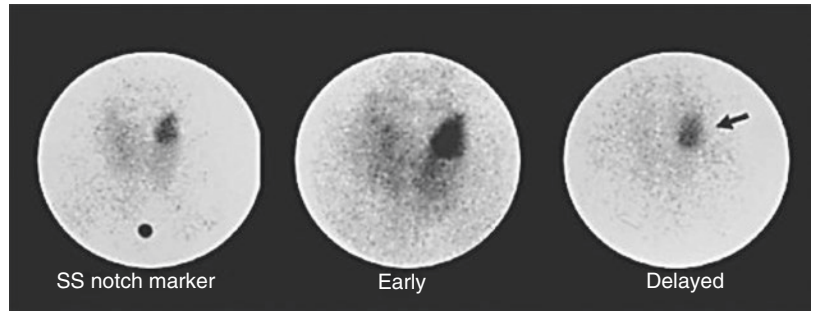

Fig. 6.12 ^{99m}Tc-sestamibi study acquired 15–90 min post injection using pinhole collimator. The delayed image shows differential clearance of activity from the thyroid gland with retained and intense uptake by a large parathyroid adenoma (*arrow*)

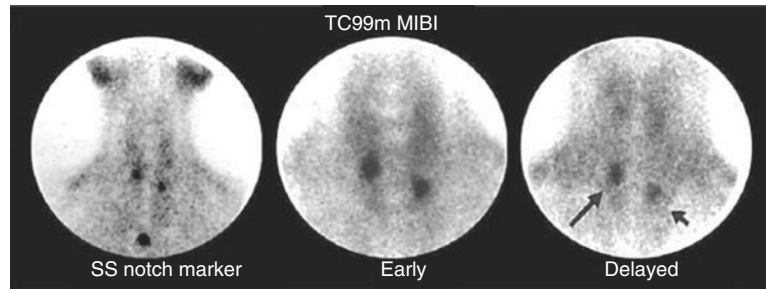

Fig. 6.13 Hyperplastic parathyroid glands (*arrows*) with persistent uptake on delayed ^{99m}Tc-sestamibi image

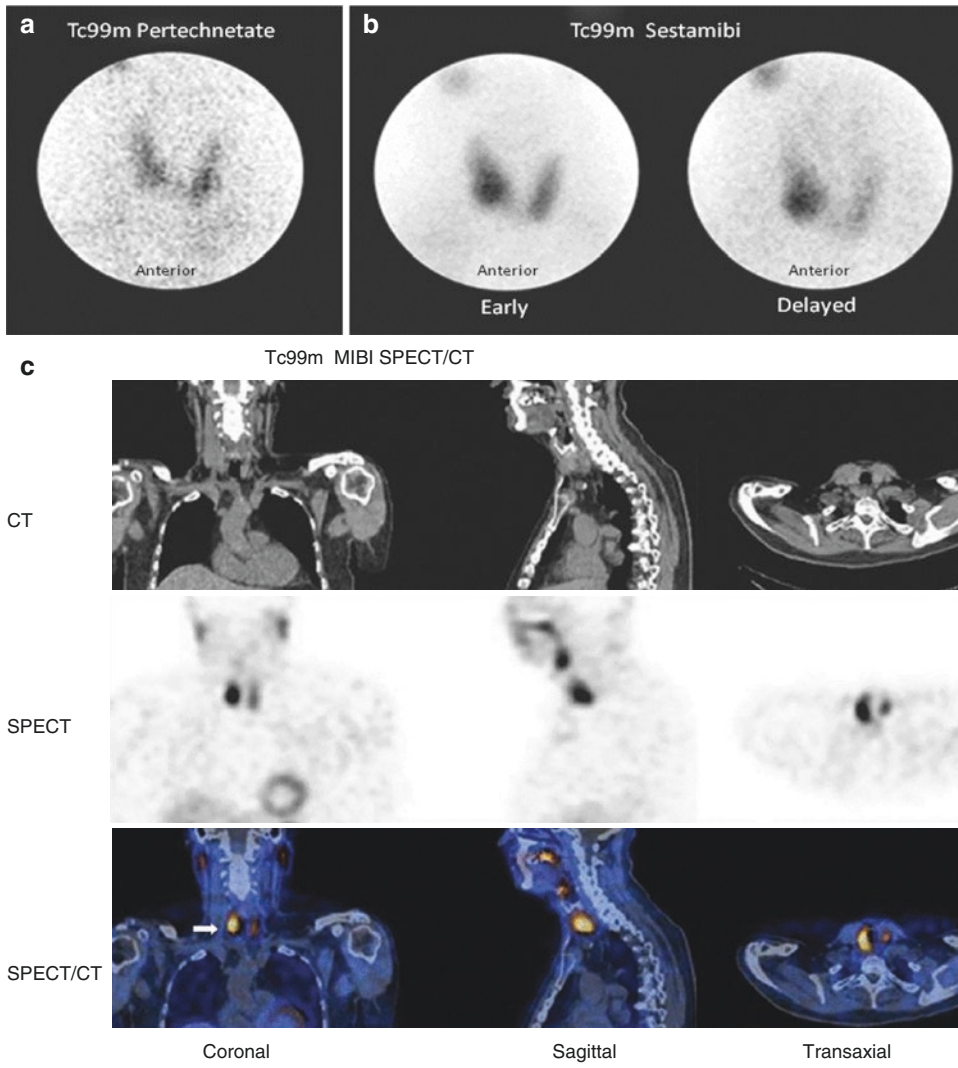

Fig. 6.14 A 70-year-old male with osteoporosis who is on rheumatoid arthritis treatment. He has hypercalcemia and high parathyroid hormone (PTH) levels. Tc-99m pertechnetate thyroid scan (**a**) and Tc-99msestamibi planar (**b**) with SPECT/CT (**c**) were performed. The thyroid scan (**a**) is grossly normal with no focal abnormalities. There is a focus of increases uptake on early sestamibi image (**b**) in the region of the right lower pole of the thyroid which does not show significant washout of activity and becomes more prominent on delayed image. There is normal washout of activity from the thyroid gland. Based on planar images, scintigraphic findings are consistent with parathyroid adenoma at the region of the right lower pole. Selected SPECT/CT images (**c**) demonstrate that this focal activity is located posterior to the lower pole of the right lobe (arrow). Note that SPECT/CT better located the lesion as compared to planar imaging

^{18}F-fluorocholine (FCH) PET/CT, correctly detected 96% and 90%, on a per patient-based and per lesion-based analysis, respectively [110].

6.2.10 Atypical Washout of Radiotracer

As outlined, the diagnosis of parathyroid tumor with MIBI scintigraphy is based on the differential washout rate between the thyroid and diseased parathyroids. Atypical radiotracer clearance whether fast parathyroid or delayed thyroid gland washout will limit the efficacy of detection of parathyroid disease with dual-phase MIBI scintigraphy as well as using the intraoperative probe.

Early parathyroid washout is frequently seen in parathyroid hyperplasia; the detection rate for this entity is approximately half of that for parathyroid adenoma [92]. Scintigraphy performs worse in cases of multisite hyperplasia, in which only the most prominent radiotracer-avid gland is visualized. In addition, rapid washout from a parathyroid adenoma has been attributed, without unanimous confirmation, to the histological composition of the adenoma [92]. Modifying the imaging protocol with additional interval scanning between the standard 15-min and 2–4-h acquisitions may be helpful in demonstrating rapid washout.

Delayed radiotracer washout from the thyroid parenchyma makes dual-phase scintigraphic assessment difficult. It was observed that the delay varies, and significant washout may not occur even several hours after injection of the radiotracer. This retention of MIBI occurs in thyroid diseases such as multinodular goiter, Hashimoto's thyroiditis, thyroid adenoma, and thyroid carcinoma owing to the hypermetabolic characteristics of these diseases [93]. Extended delayed-phase imaging of MIBI along with in-depth clinical examination may be useful in the diagnosis of concomitant thyroid and parathyroid disease.

As rapid washout and small size of parathyroid glands would cause false-negative localization studies, several pathologies can also cause false-positive studies (Table 6.8).

Table 6.8 Causes of false-positive MIBI parathyroid studies

Lymph nodes
Supraclavicular
Axillary
Hyperplastic thymus[a]
Sarcoidosis[b]
Carcinoid tumor
Malignant tumors

[a] Confused with an intrathymic or mediastinal parathyroid adenoma
[b] Thorax

6.2.11 Intraoperative Probe Localization

Localization using intraoperative gamma probe has recently gained popularity. The patient is injected 2 h before surgery, and the probe is used to detect the higher level of activity after exploration by the surgeon. On the day of surgery, the patients receive the same dose of MIBI as for imaging and is taken to the operating room. Prior to skin incision, counts over four quadrants in the neck as well as over the mediastinum are obtained using a gamma probe.

6.3 Adrenal Gland

6.3.1 Anatomical and Physiological Considerations

The adult adrenal glands weigh 8–10 g and lie above and slightly medial to the upper pole of both kidneys. The outer cortex comprises 90% of the adrenal weight, the inner medulla about 10%. The cortex is rich with vessels and receives its main blood supply from branches of the inferior phrenic artery, renal arteries, and the aorta. These small arteries form an arterial plexus beneath the capsule and then enter a sinusoid system that penetrates the cortex and medulla, draining into a single central vein in each gland [111].

Histologically, the adult adrenal cortex is composed of three zones: an outer zona glomerulosa which produces aldosterone, a zona fasciculata, and an inner zona reticularis. The zona fasciculata is the thickest layer and produces cortisol and androgens; its cells are large and contain

more lipid and thus are termed clear cells. The zona reticularis produces weak androgens. The zonae fasciculata and reticularis are regulated by adrenocorticotropic hormone (ACTH).

Cholesterol within the adrenal cortex is the starting point for synthesis of multiple adrenal hormones. Therefore, a radioactive cholesterol is useful in evaluating the functional status of adrenocortical lesions The adrenal medulla is composed histologically of chromaffin cells, which are large ovoid columnar cells arranged in clumps or cords around blood vessels and surrounded by capillaries and sinusoids. They have large nuclei and a well-developed Golgi apparatus; they have a large number of granules containing catecholamines. The adrenal medulla also contains some sympathetic ganglia. The cells of adrenal medulla are innervated by preganglionic sympathetic fibers. Most of the blood supply to the hormonally active cells of the medulla is derived from a portal vascular system arising from the capillaries in the cortex. There is also a network of lymphatics that drain into a plexus around the central vein [112]. The adrenals provide adjustment of heart performance and vascular tone. Epinephrine is found essentially only in the adrenal medulla, and constituting greater than 80% of its output. Norepinephrine is synthesized by adrenergic neurons and cells of the adrenal medulla; therefore, a radioactive norepinephrine analog is used to evaluate adrenomedullary lesions.

6.3.2 Adrenal Cortex

6.3.2.1 Pathophysiology

Primary Aldosteronism (Conn's Syndrome)

In primary aldosteronism (Conn's syndrome), there is increased production of aldosterone by abnormal zona glomerulosa (adenoma or hyperplasia) leading to hypertension through the increased reabsorption of sodium and water from the distal tubules. A benign adenoma accounts for 75% of cases of this syndrome; it is usually small, ranging from 0.5 to 1.5 cm in diameter. It is more common in women than in men (3:1) and usually occurs between the ages of 30 and 50 years. Bilateral, or rarely unilateral, micro- or macronodular adrenal hyperplasia accounts for most of the remaining cases. Two types of familial hyperaldosteronism have recently been identified: Type I is glucocorticoid suppressible and associated with bilateral hyperplasia, and type II is associated with adrenocortical adenoma. Adrenal carcinoma is a very rare cause of this syndrome. The patients typically come to medical attention because of clinical signs of hypokalemia or detection of previously unsuspected hypertension during the course of a routine physical examination. The diagnosis is principally a biochemical one (low plasma renin activity and a high level of aldosterone); imaging is required to localize the lesion and identify its multiplicity. The diagnostic information provided by CT or MRI in localizing adenomas is both accurate and practical, and they are the initial approach of choice. Some smaller adenomas which are not clearly visualized by CT can be depicted by scintigraphy.

Cushing's Syndrome

The most common pathological cause of this syndrome is the stimulation of the zona fasciculata by excess ACTH from the pituitary gland (Cushing's disease) or, less commonly, the ectopic production of ACTH (as in small cell lung cancer and neural crest tumors) or corticotropin-releasing factor (CRF) (as in bronchial carcinoid and prostate cancer). Stimulating this zona may lead to bilateral adrenocortical hyperplasia, which is nodular in 25% and diffuse in 75% of cases. Cushing's syndrome may also be due to autonomous adrenal cortisol production (30–40% of cases) due to adrenal adenoma or hyperfunctioning adrenal carcinoma. ACTH-induced Cushing's disease is more common in adults (25–45 years) and is at least three times more common in women than in men. Cushing's disease resulting from ectopic ACTH secretion is more common in older adults, particularly men. Adrenal tumors rather than pituitary tumors are more common in children, especially girls. Twenty percent of nonfunctional adrenocortical carcinomas tend to be highly malignant, with weights exceeding 1 kg.

Hyperandrogenism

Hyperandrogenism can be the result of hypersecretion of androgens (causing virilization) or estrogens (causing feminization) from the zona reticularis of the adrenal cortex by primary adrenocortical hyperplasia and rarely by adrenal tumors, though the most common cause of this syndrome is polycystic ovary disease (POD). In POD, the chronic anovulation associated with increased circulating LH levels results in increased ovarian stromal stimulation, which leads to increased ovarian androgen production. A testosterone-secreting adrenal adenoma may contain the crystalloids characteristic of Leydig's cells [113].

6.3.2.2 Scintigraphy

Radiolabeled Cholesterol Analogs

NP(^{131}I-7-iodomethyl-19-norcholesterol)-59 (NP-59) is the classic nuclear medicine study used to evaluate some disease processes related to the adrenal cortex. Its main uses are documented cases of adrenal excess secretion and negative or equivocal CT or MRI findings. This radiopharmaceutical is a cholesterol analog that is bound to and transported by low-density lipoproteins (LDL) to specific LDL receptors on adrenocortical cells; therefore, endogenous hypercholesterolemia may limit the number of receptors available for radiocholesterol localization through competitive inhibition. Once liberated from LDL, NP-59 is esterified but is not further converted to steroid hormones [114]. This scan should be done only on patients with clinically hyperfunctioning adrenal cortex verified by lab results, CT, or MRI.

Patient Preparation

1. Suppression of normal adrenal cortex is achieved by oral administration of 1 mg dexamethasone q.i.d. beginning 7 days before and for the duration of the study. This is not required in patients with hypercortisolism.
2. Stop diuretics, spironolactone, and antihypertensive drugs, if feasible for at least 48 h.
3. Saturated solution of kalium iodide (SSKI) is given orally in a dose of one drop t.i.d. starting 2 days before and continuing for 14 days to suppress the thyroid uptake of free radioiodine. Patients allergic to iodine can take potassium perchlorate (200 mg every night after meals), starting 1 day before injection of NP-59, for 10 days.
4. A laxative should be given starting 48 h prior to imaging and continuing till final imaging to diminish bowel activity. Enemas may be required. The dose of ^{131}I-NP-59 is 1 mCi, to be strictly injected i.v. through a secured i.v. line over 2 min. NP-59 background clearance and accumulation in the adrenals occur slowly, but by day 5, accumulation in the normal adrenals is greater than in other organs. Suppressed patients should be imaged on days 3, 4, 5, and 7. If the adrenals are not seen by day 7, dexamethasone should be stopped and the patient imaged on day 10; nonsuppressed patients are imaged on days 5 and 7. Anterior and posterior projections of the adrenals are obtained; in case of hyperandrogenism, the pelvis and genitalia should be included.

The normal distribution is seen in the liver, gallbladder, and colon. In 90% of cases, the right adrenal gland is more cephalad and deeper than the left adrenal gland. In two-thirds of normal subjects, the activity in the right adrenal appears greater than that in the left in the posterior projection; this is because the right adrenal occupies a more posterior location than the left adrenal. In some instances, the gallbladder can be confused with the right adrenal. In the lateral view, the gallbladder is located anteriorly. In difficult cases, cholecystokinin can clear the gallbladder activity. Interfering colonic activity can be reduced by cathartics. Although count rates are low, single photon-emission computed tomography (SPECT) can be performed and may separate adrenals from gut and liver activity.

In primary aldosteronism, early unilateral increased uptake indicates adrenal adenoma, whereas bilateral increased uptake suggests bilateral adrenal hyperplasia. Pituitary ACTH-producing adenoma or ectopic ACTH secretion

can result in bilateral adrenal hyperplasia manifested by bilateral symmetric increased uptake, with ectopic causes producing more uptake of NP-59; this pattern may be asymmetric in the macronodular form of hyperplasia. Adrenal adenoma causes unilateral increased uptake, whereas adrenocortical carcinoma gives rise to bilateral nonvisualization. In hyperandrogenism, early bilateral uptake is compatible with hyperplasia, and early (<5 days) unilateral uptake or markedly a symmetric visualization is indicative of adrenal adenoma.

Positron Emission Tomography Imaging

Since adrenal adenomas are relatively common (2–9%) in the general population, incidental detection of adrenal lesions poses a diagnostic challenge, particularly in patients with a previous clinical history of malignancy [115, 116].

CT is used as the first-line diagnostic modality for screening and determining the nature of the adrenal lesions, and MRI is often performed to further characterize indeterminate masses seen on CT. ^{18}F-FDG PET can help in differentiating malignant from benign adrenal lesions in patients with proven malignancy or in patients with incidentally detected adrenal tumors on CT or MRI studies [116–118]. However, some adenomas show increased FDG tracer uptake similar to cancer and some do not. It has been suggested that the functional state of an adenoma is a factor determining the intensity of uptake, with $^{18F\text{-}FDG}$ uptake being increased in functioning adrenal masses [119]. SUV value can help differentiate adrenal cortical adenomas from adrenal cortical carcinomas [118].

Specific inhibitors of adrenal steroidogenesis, etomidate and metomidate, have recently been used to develop suitable PET tracer. These molecules seem to be suitable as in vivo tracers for specific visualization of the normal adrenal cortex and positive identification of adrenocortical tumors. To date adrenocortical radiocholesterol scintigraphy has been shown to be the most accurate noninvasive imaging technique in differentiating benign cortical adenomas from space-occupying or destructive adrenal lesions.

6.3.3 Adrenal Medulla

6.3.3.1 Pathophysiology

Neuroendocrine tumors are a heterogeneous group of usually slow-growing tumors that arise from neuroendocrine cells from various organs, including adrenal in addition to lung, thymus, thyroid, stomach, duodenum small bowel, large bowel, appendix, pancreas, and skin (see Chap. 12).

Pheochromocytoma

Pheochromocytoma is a rare tumor arising from chromaffin cells of the adrenal medulla. Most pheochromocytomas produce excessive amounts of norepinephrine, attributable to autonomous functioning of the tumor, although large tumors may secrete both norepinephrine and epinephrine [120] and in some cases also dopamine. The release of catecholamine into the circulation causes hypertension, tremor, tachycardia, and other signs. Other catecholamine-producing tumors (e.g., chemodectoma and ganglioneuroma) may also cause a syndrome similar to that seen with pheochromocytoma. Furthermore, they may also produce some active peptides such as somatostatin, ACTH, and calcitonin.

Pheochromocytomas vary in size from less than 1 g to several kilograms; in general, they are small, most weighing under 100 g. They are vascular tumors, tend to be capsulated, and commonly contain cystic or hemorrhagic areas. The cells tend to be large and contain typical catecholamine storage granules. Multinucleated cells, pleomorphic nuclei, mitosis, and extension into capsule and vessels are sometimes seen but do not indicate that the tumor is malignant. The chromogranin existing within secretory granules in the tumor tends to form *Zellballen* (cell balls); these structures are surrounded by sustentacular cells. Five to ten percent of cases are malignant, and malignancy is determined by the only biological behavior of the tumor. It is estimated that 0.1% of hypertensive patients have pheochromocytoma. More than 90% of patients with pheochromocytoma exhibit hypertension, which is sustained in two-thirds of patients. These tumors are observed

more frequently in women than in men and at all ages, including infancy; they are most common in the fifth and sixth decades [120].

Although most patients with functioning tumors have symptoms (sweating, palpitation, headache, dyspnea, and anxiety), most of the time, these vary in intensity, and in about half of the patients, they are paroxysmal. Pheochromocytomas are usually sporadic, but about 10–20% of cases are familial and arise alone or as part of several hereditary syndromes including multiple endocrine neoplasia (MEN) type IIa and type IIb, neuroectodermal disorders (tuberous sclerosis, von Hippel–Lindau disease, and neurofibromatosis type I), Carney's syndrome (pulmonary chondroma, gastric epithelioid leiomyosarcoma, and paraganglioma), and McCune–Albright syndrome. Pheochromocytoma can be found anywhere in the sympathetic nervous system from the neck to the sacrum; it is subdiaphragmatic in about 98% of cases. In 85–90% of these cases, it is found in the adrenal medulla. In sporadic cases of pheochromocytoma, 80% of the tumors are unilateral, 10% bilateral, and 10% extra-adrenal (paraganglioma). In contrast, two-thirds of those occurring in the context of MEN are bilateral. In children, it is extra-adrenal in 30% of cases. These extra-adrenal locations are para-aortic sympathetic chain (8%), organ of Zuckerkandl at origin of the inferior mesenteric artery (2–5%), and gonads, scrotum, and urinary bladder (1%). Fewer than 10% of these tumors are malignant and metastasize by lymphatic or hematogenous routes; metastases are usually found in the skeleton, liver, lymph nodes, and lungs [121]. The differential diagnosis includes thyrotoxicosis, migraine, sympathomimetic drug use, menopausal hot flushes, and anxiety disorders. Patients with persistent symptoms and hypertension may develop complications such as nephropathy, retinopathy, myocardial infarction, cerebrovascular accidents, and congestive heart failure.

The diagnosis is confirmed by assay of catecholamines and their metabolites, followed by MRI or CT to localize the lesion; predominant production of epinephrine, when present, suggests an adrenal location. Dopamine excretion is a sensitive indicator of tumor aggressiveness, and a rising plasma or urinary dopamine level is regarded as a poor prognostic indicator.

MRI is somewhat more successful in locating extra-adrenal tumors and has the advantage of providing bright images of pheochromocytoma with T_2 weighting in contrast to most other adrenal tumors. Only the smallest tumors or those shielded by clips and other metal objects from previous surgery cannot be detected; in these cases, an MIBG study is indicated.

Neuroblastoma

Neuroblastoma is a malignant tumor of the sympathetic nervous system, accounting for up to 10% of childhood cancers and 15% of cancer deaths among children. Seventy-five percent of neuroblastoma patients are younger than 4 years. The tumor is usually more than 5 cm in the largest diameter and tends to extend across the midline; it has the potential to mature into pheochromocytoma or ganglioneuroma. Metastases are the first manifestation in up to 60% of cases. The electron microscopic appearance of NB cells is distinctive. The malignant neuroblasts exhibit peripheral dendritic processes containing longitudinally oriented microtubules, neurosecretory granules, and filaments in the cytoplasm. Neuroblastomas readily infiltrate the surrounding structures and metastasize to the regional lymph nodes, liver, lungs, and bones; metastases to the orbit may result in proptosis [122]. Areas of necrosis, hemorrhage, calcification, and cystic changes are frequently present. Around one-third of cases are found in the adrenal gland, another third in other abdominal sites, and 20% in the posterior mediastinum. More than 90% of these tumors produce catecholamine in excess, but they rarely cause typical clinical syndromes. Severe diarrhea may be caused by secretion of vasoactive intestinal peptides by the neuroblastoma.

Ganglioneuroma

Ganglioneuroma is a benign tumor found in older children and young adults, with no sex predilection. Forty percent of the patients are over 20 years of age. Up to 30% of these tumors occur in the adrenal medulla and 43% in the posterior

mediastinum. Histologically, the tumor consists of mature ganglion cells and is well encapsulated; it is frequently calcified and rarely hormone active.

6.3.3.2 Scintigraphy

Metaiodobenzylguanidine

Metaiodobenzylguanidine (MIBG) is a guanethidine analog chemically similar to noradrenaline. Following i.v. injection, MIBG is rapidly cleared from the vascular compartment; however, a small amount remains in the thrombocytes. It localizes in storage granules of adrenergic tissue (referred to as synaptosomes) by means of energy- and Na-dependent mechanisms (type 1), and it is not metabolized to any appreciable extent. Neural crest tumors have these synaptosomes in abundance.

Preparation. The patient should be given Lugol solution orally (3 drops b.i.d. for 4–5 days, starting 2 days before injection to block the thyroid uptake of free ^{131}I. The patient should stop taking reserpine, imipramine, calcium channel blockers, cocaine, labetalol, amphetamine-like drugs, and others.

The dose of ^{131}I-MIBG is 0.5–1.0 mCi and results in a radiation dose of 50–100 rads/mCi to the adrenal medulla. The dose of ^{123}I-MIBG is 3–10 mCi, with a radiation dose of 0.80 rads/mCi to the adrenal medulla. The normal distribution of ^{123}I-MIBG is to the salivary gland, liver, urinary bladder, gastrointestinal tract, lung, myocardium, normal adrenal gland, thyroid, spleen, and uterus [123–126]; in small children, uptake may also be seen in the nape of the neck, which is currently believed to be related to accumulation in brown adipose tissue [127].

Eighty-five percent of the injected dose is excreted unchanged by the kidneys. Imaging is performed at 24 and 48 h after injection of ^{131}I-MIBG and at 6 and 24 h after injection of ^{123}I-MIBG (Fig. 6.15). When SPECT is used (Figs. 6.16 and 6.17), increased certainty is achieved in interpreting the studies [124]. It is worthy of mention that ^{123}I is better than ^{131}I,

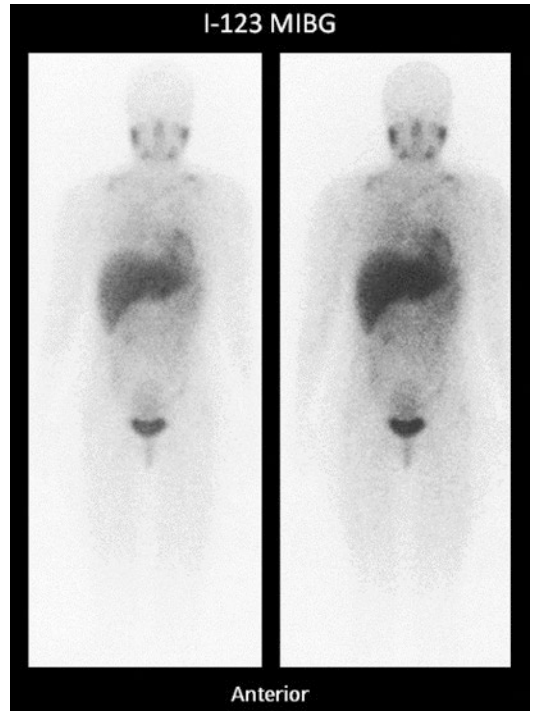

Fig. 6.15 A 32-year-old male with suspected pheochromocytoma. Anterior ^{123}I-MIBG whole-body image with different intensity is shown. There is increased uptake at the supraclavicular region bilaterally. This pattern is due to uptake by brown fat. The remainder of the study shows also physiological distribution of the radiotracer with no abnormalities

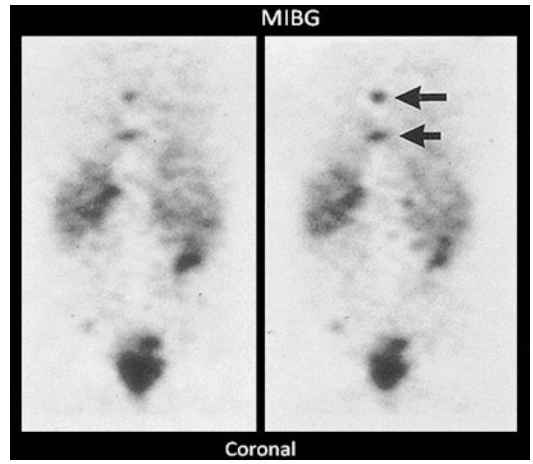

Fig. 6.16 Representative coronal images from a SPECT ^{131}I-MIBG study for a patient with neuroblastoma, showing metastases to the spine (*arrows*)

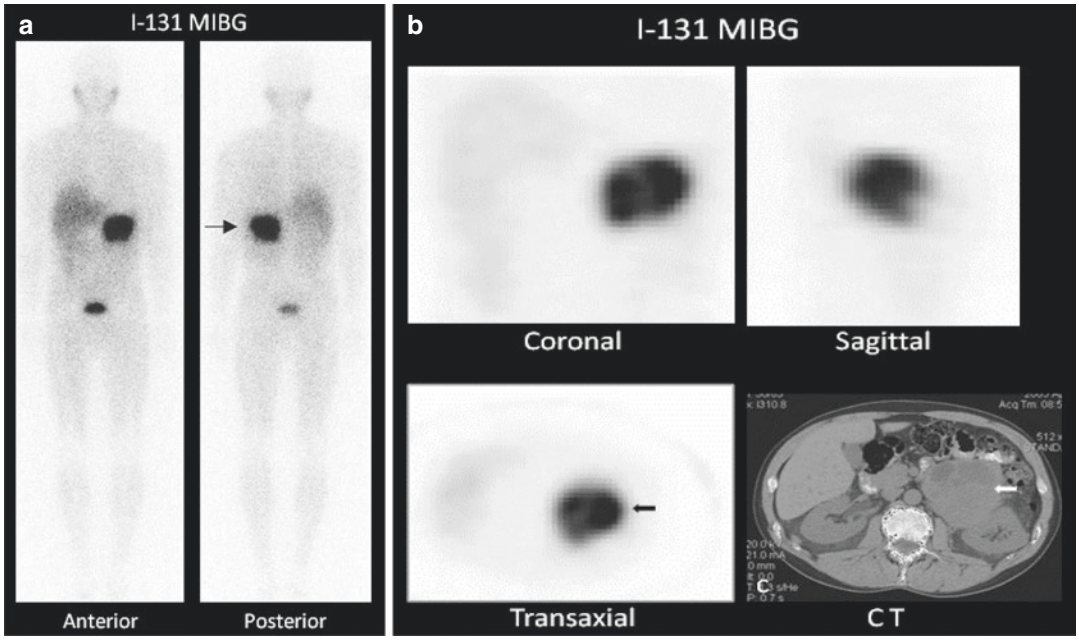

Fig. 6.17 A planar (**a**) and SPECT (**b**) ^{131}I-MIBG study and a CT section of a patient with a large pheochromocytoma (*arrow*s)

especially in the pediatric population, because of the lower radiation exposure to the adrenals in addition to the superior image quality of the former. The sensitivity of ^{131}I-MIBG in pheochromocytoma is 80–90% and specificity is more than 90%; positive MIBG uptake in benign solitary pheochromocytoma occurs in about 90% of patients [128]; tumors as small as 1–2 cm in diameter were detected especially with ^{123}I [129].

Moreover, metastatic and recurrent tumors can also be located (Figs. 6.17 and 6.18). Adrenal medullary hyperplasia found in MEN IIa is difficult to diagnose with CT or MRI. MIBG scintigraphy is uniquely suited to detect this condition. Occasionally, however, some large tumors are not visualized because of extensive tumor necrosis.

MIBG is localized in other neuroendocrine tumors to a lesser degree, including carcinoid, medullary thyroid carcinoma, and paraganglioma. Indium-111 octreotide (a somatostatin analog) is less accurate in the detection of pheochromocytoma, probably due to normal physiological uptake in the liver, spleen, and kidneys and blocking of somatostatin receptors by endogenous somatostatin.

Radiolabeled MIBG imaging is now a well-established examination in the diagnostic evaluation of neuroblastoma. ^{123}I is preferred especially in pediatric patients (dose 3–5 mCi) due to its favorable dosimetry and superior image quality; scintigraphy can be performed as early as 4 h after injection. Elevated catecholamine levels are not necessary for the detection of NB by MIBG. The sensitivity of MIBG in NB is 91%. Somatostatin analog scintigraphy has been reported to visualize MIBG-negative tumor sites in patients with NB. MIBG is essentil [130] as a prelude to ^{131}I-MIBG therapy. In the follow-up of the patients with high-risk neuroblastoma, SPECT/CT MIBG has been found to improve significantly the imaging interpretation and provides positive impact on patient management [131]. Recently, the use of low-dose ^{124}I-MIBG PET/CT for monitoring neuroblastoma in children and evaluating tumor burden showed better tumor detection capability compared to ^{123}I-MIBG planar imaging and SPECT/CT [131].

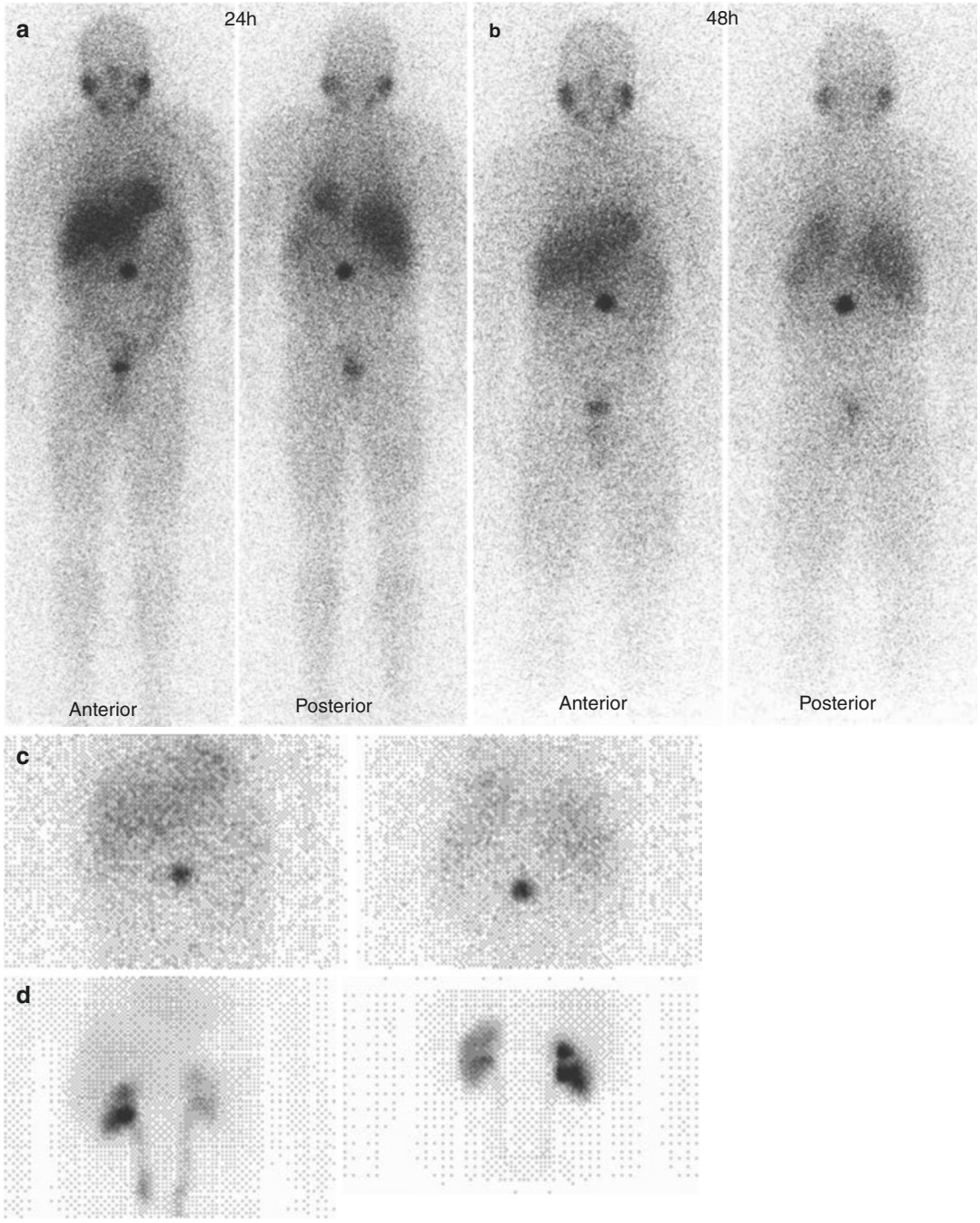

Fig. 6.18 ^{123}I-MIBG whole body (**a**, **b**) of a patient with known pheochromocytoma who was referred for back pain. The study shows a focal area of increased uptake in the midline of the abdomen. Forty-eight hours spot image (**c**) was acquired, and 99mTc-DTPA study (**d**) was also obtained for comparison and lesion appeared away from the kidneys. The study was correlated with 99mTc-MDP spot images of the thoracolumbar spine (**e**) which showed questionable focal abnormality in the midlumbar spine corresponding to the location of I-123 abnormal uptake. MRI (**f**) and CT (**g**) scans were obtained and show a lesion in L-3 representing metastatic pheochromocytoma

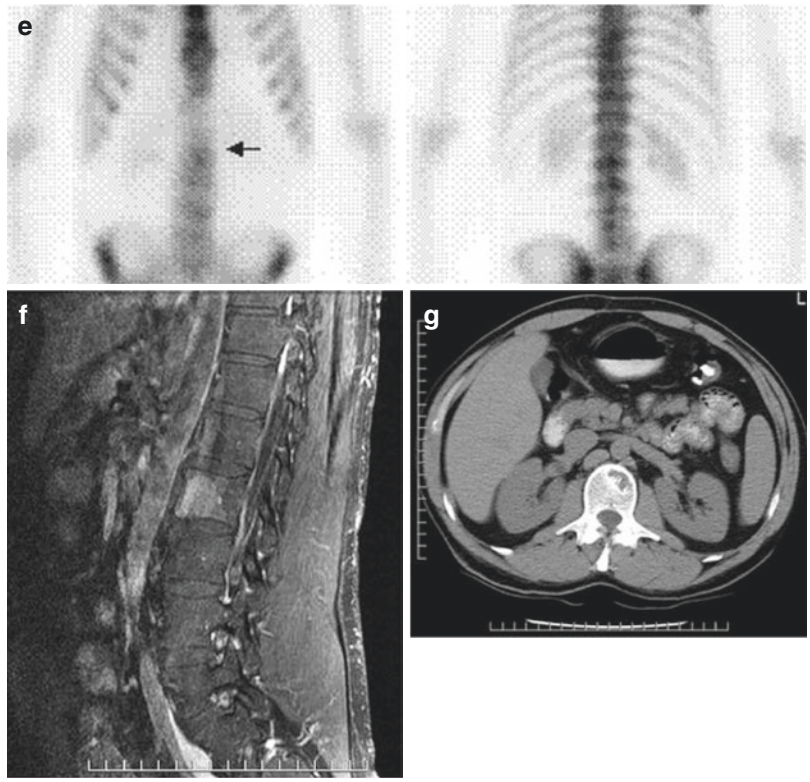

Fig. 6.18 (continued)

Other PET agents are also being used since approximately 10% of the neuroblastomas are non MIBG avid [132].

Indium-111 Octreotide

In healthy human beings, somatostatin, a natural neuropeptide, is produced in various tissues, including the nervous system, endocrine pancreas, and gastrointestinal tract. Somatostatin inhibits the secretion of several hormones, most importantly GH and TSH.

Neuroendocrine (including adrenal medulla) and non-neuroendocrine organs have surface receptors that bind to somatostatin. Octreotide, a somatostatin analog with a half-life of 120 min, is used to evaluate the tumors that contain these receptors, in which case it binds to somatostatin receptor subtypes 2 and 5. Among these tumors are pheochromocytoma, neuroblastoma, paraganglioma, and others including pancreatic tumors and carcinoid.

Octreotide is usually tagged with ^{111}In (Fig. 6.19), although ^{123}I has also been used in the past. It is recommended that octreotide therapy be withheld for at least 72 h prior to the injection of the radiopharmaceutical. Following i.v. injection of a standard dose of 6 mCi, static images are obtained at 4 and 24 h (Fig. 6.19). SPECT images through the region of interest are then obtained at 4 h and at 24 h if needed. This radiopharmaceutical is excreted via glomerular filtration. In a normal patient, octreotide activity is identified in the thyroid, kidneys, liver, spleen, pituitary, gallbladder, and, to a lesser extent, the bowel on delayed images. The kidney and spleen receive the highest absorbed dose. A focal area of intense early radiotracer uptake is considered to be pathological, indicating primary neoplasm or metastasis. A false-negative scan is seen in cases where the tumor is small, has few somatostatin receptors, or both. ^{111}In-octreotide scanning is highly sensitive for

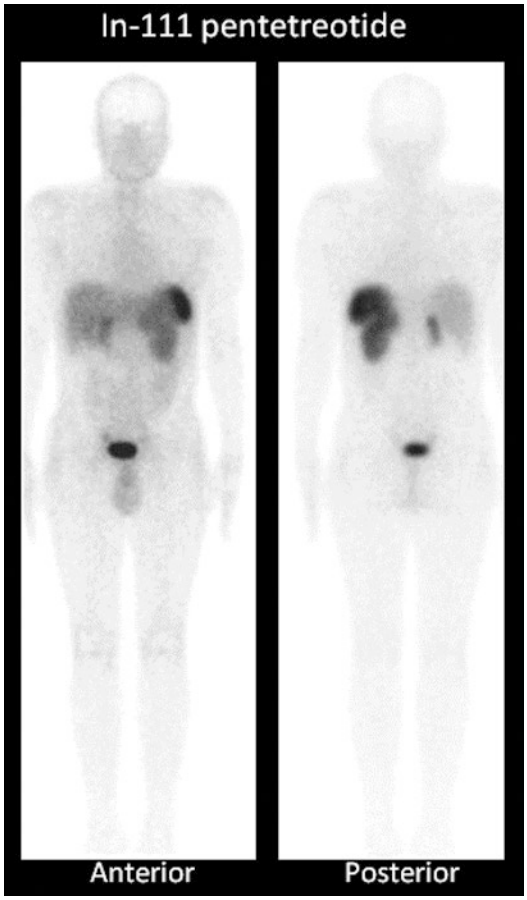

Fig. 6.19 Normal distribution of In-111 pentetreotide includes intense uptake in the spleen as well as uptake in the liver and activity in the kidneys and urinary bladder. Bowel activity is seen usually at 24 h. The pituitary and the thyroid glands may be faintly visualized. Biliary excretion of the tracer occurs with occasional visualization of the gallbladder. Note that the right kidney is smaller than the left in this case

detecting tumors greater than 1.5 cm. Since the expression of somatostatin receptors in neuroblastomas is variable with less receptors in more advanced disease, an accurate sensitivity of ^{111}In-octreotide is not readily definable. In children, several studies have compared ^{111}In-octreotide with MIBG scintigraphy for imaging neuroblastoma; the sensitivity of the former ranged from 55 to 70% and that of the latter 83–94% [133–137]. Several studies reported MIBG-negative tumor sites detected by ^{111}In-pentetreotide in patients with neuroblastomas [133–137]. High affinity of octreotide for the MIBG-negative neuroblastoma cell line has been found. Tenenbaum et al. recommended the use of octreotide to detect somatostatin receptors when results from MIBG scans are negative [134]. Pashankar suggested that neuroblastoma can be imaged by either ^{111}In-octreotide or MIBG depending on local expertise, as they have a complementary role in the initial diagnostic workup particularly since ^{111}In-octreotide additionally correlates with prognosis [136] (Figs. 6.20 and 6.21).

^{111}In-octreotide is currently the agent of choice for nuclear medicine imaging of head and neck paraganglioma, though it is insensitive for lesions less than 1 cm. The recent introduction of SPECT/CT has greatly improved the sensitivity of ^{111}In-octreotide scintigraphy [138].

It was suggested that ^{111}In-DTPA-D-Phe-1--octreotide might be useful for radiation therapy of patients with surgically incurable tumors having high somatostatin receptor densities such as carcinoid [139].

Positron Emission Tomography Imaging

PET has been used to evaluate adrenal masses. The higher spatial resolution of PET scanners (Figs. 6.22, 6.23, and 6.24) enables the detection of small tumors not seen with ^{123}I-MIBG. Malignant adrenal tumors can be detected with FDG PET, but its use in these cases is limited due to the low specificity. FDG PET/CT can help detect certain malignant lesions particularly the minority which are not detected by MIBG. ^{11}C-hydroxyephedrine, the first available positron-emitting tracer of the sympathetic nervous system, was found useful in the detection of pheochromocytomas, with a high level of accuracy [141]. Its uptake reflects catecholamine transport and storage and neuronal reuptake. In detecting metastatic pheochromocytomas, (^{18}F) dopamine was found to be a superior to ^{131}I-MIBG [142–144]. PET imaging is used for the detection, localization, staging, and follow-up of neuroendocrine tumors. It can also be used to determine SSTR status of the tumor and for selecting patients

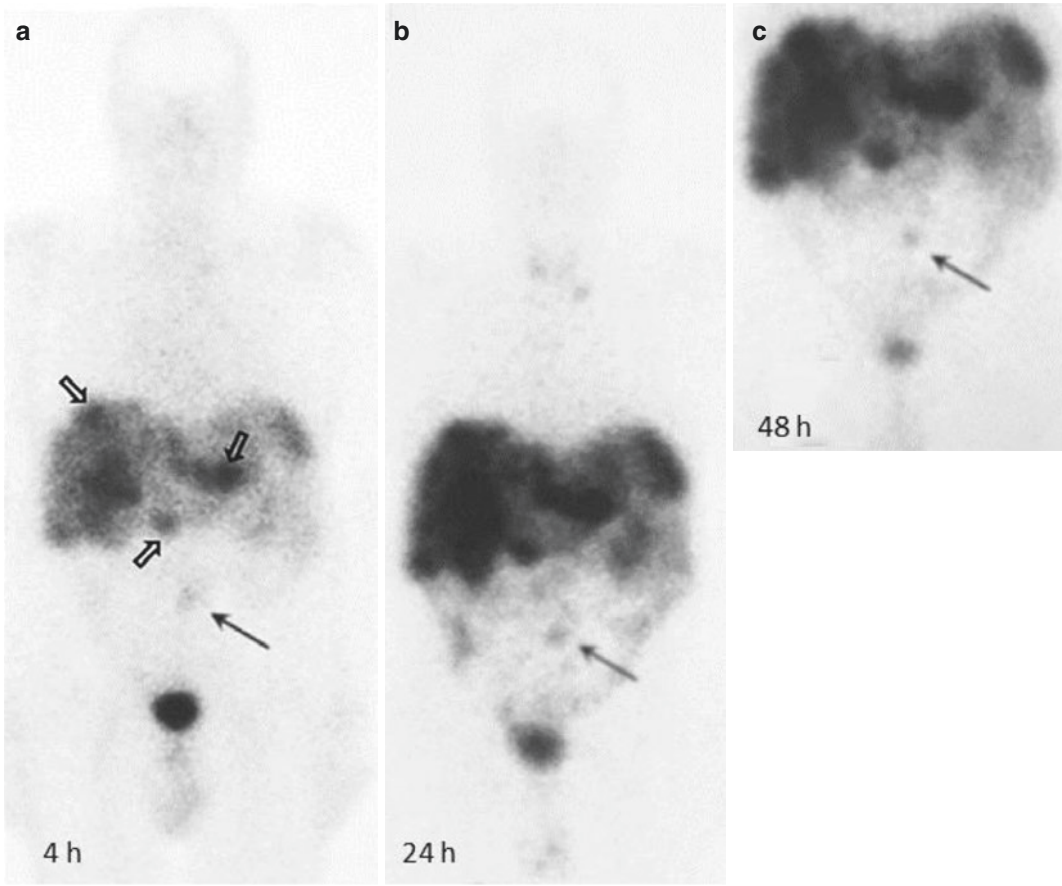

Fig. 6.20 ^{111}In-octreotide imaging study obtained at 4 (**a**), 24 (**b**), and 48 (**c**) h after i.v. injection of 6 mCi of the radiopharmaceutical. The images illustrate—in addition to the foci of metastatic carcinoid to the liver—the physiological uptake in the liver, spleen, kidneys, bowel, and urinary bladder. Note that delayed imaging (**c**) and/or SPECT may be needed to differentiate physiological activity such as in the bowel from true disease (*arrow*) such as in this case

with metastatic disease for SSTR radionuclide therapy with Lutetium-177 (Lu-177)- or Yttrium-90 (Y-90)-labeled somatostatin analogs. 68-Ga-DOTATATE and 64-Cu-DOTATATE are radiolabeled somatostatin analogs for the diagnosis and pretreatment evaluation of neuroendocrine tumors with PET.

PET imaging with Ga-68 DOTA peptides is more accurate and detects more lesions than Octreoscan in carcinoid tumors and other neuroendocrine tumors [142]. Figures 6.22 and 6.23 illustrate normal and abnormal Ga-68 DOTA TATE studies.

6.3.4 Incidental Adrenal Mass

Incidental detection of adrenal lesions is a diagnostic challenge since adrenal adenomas are relatively common (2–9%) in the general population. This is particularly important in patients with a previous clinical history of malignancy. Incidental adrenal lesions are detected in about 2–5% of contrast-enhanced abdominal CT examinations making the diagnosis of adrenal incidentaloma a common clinical problem [145]. In these cases, the patients should be screened for pheochromocytoma clinically and biochemically. Adrenal

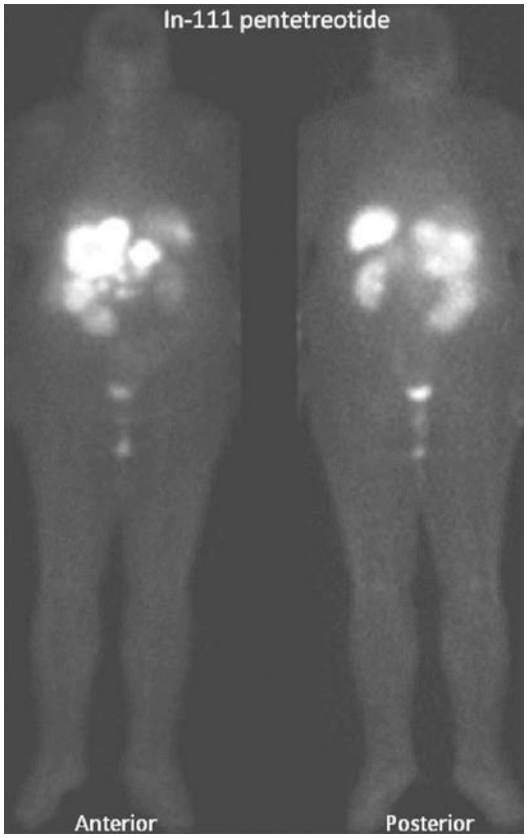

Fig. 6.21 Fifty-three-year-old female presented with carcinoid symptoms for 6 months. She was found to have metastatic disease to the liver and pancreas. In-111 pentetreotide anterior and posterior whole-body planar images at 24 h. Images reveal multiple foci of increased activity in the liver and abdomen consistent with SSTR-positive metastatic disease. SPECT/CT would better locate the abdominal disease

incidentalomas are uncommon in patients younger than 30 years but increase in frequency with age; they occur equally in males and females. Adrenocortical adenoma accounts for 36–94% of incidentalomas detected in patients without a history of malignancy [145]. Only about 10% of incidental adrenal masses are functional [145]. Accordingly, NP-59 would not be an appropriate radiotracer for adrenal incidentaloma because 90% of adrenal masses cannot incorporate NP-59 in their cells. Metomidate is an inhibitor of 11ß-hydroxylase, a key enzyme in the biosynthesis of cortisol and aldosterone by the adrenal cortex. ^{11}C-metomidate is a promising PET tracer to identify incidentalomas of adrenocortical origin [146]. Khan et al. reported on the value of ^{11}C-metomidate in evaluation of adrenocortical cancer [147].

FDG PET/CT can help detect certain malignancy in adrenal incidentalomas particularly when they occur in patients with known extra-adrenal malignancies. The prevalence of adrenal metastases discovered by FDG PET/CT has been reported to be as high as 9.9% in several studies. The upstaging resulting from FDG PET/CT can play an important role in modifying the plans of therapeutic strategies. In some patients, the adrenal metastasis can be the first manifestation of a cancer [148]. It should be noted that functional adrenal adenomas (cortisol secreting was the highest) may show increased FDG uptake in comparison to the nonfunctional adrenal masses [149].

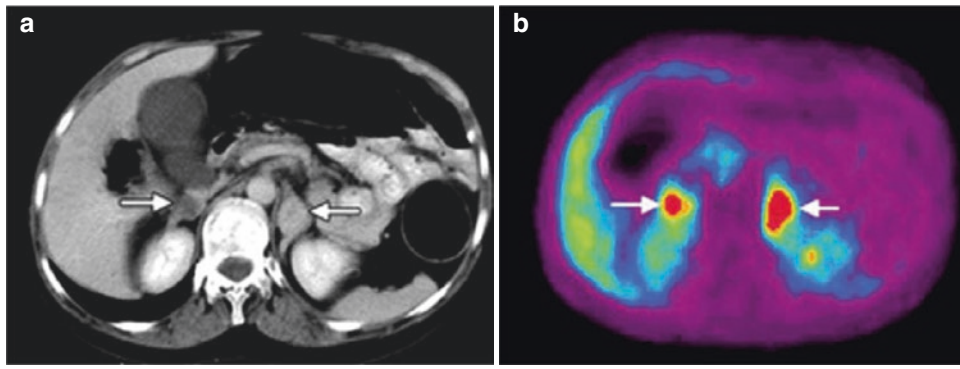

Fig. 6.22 (**a**, **b**) Transverse images obtained in a patient with multiple endocrine neoplasia type 2 and an increase in urinary catecholamine levels. A CT image shows bilateral adrenal tumors (*arrows*) and a 2-cm-diameter tumor on the right side and a 4-cm-diameter tumor on the left side adrenal lesions (*arrows*). HED PET image (**b**) shows intense uptake in both. Surgery revealed bilateral pheochromocytomas. (From Anderson et al. [140] with permission)

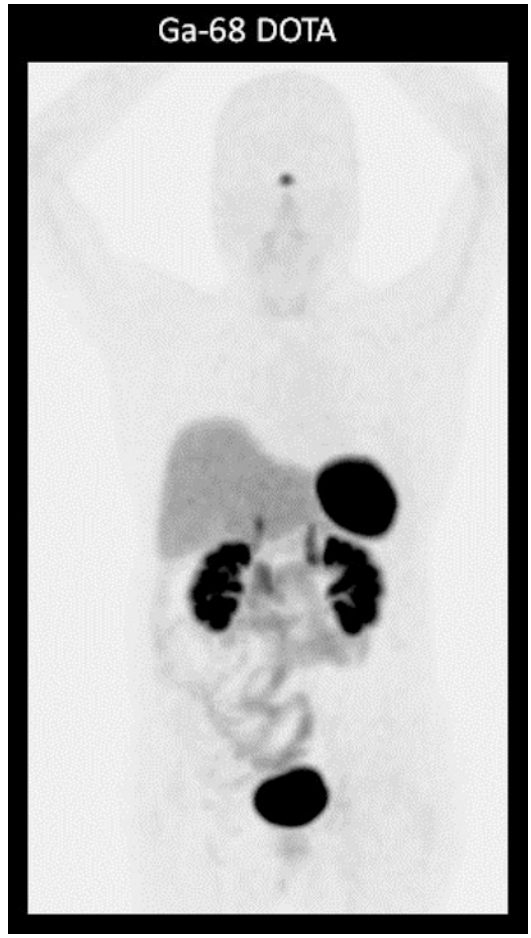

Fig. 6.23 Normal distribution of Ga-68 DOTA peptides includes intense uptake in the spleen with uptake in the pituitary gland, liver, adrenals, and pancreatic head and activity in the kidneys, bowel, and bladder. Salivary and thyroid glands show mild uptake. The prostate gland and breast glandular tissue may show diffuse low uptake. Physiological uptake in the pancreatic head may mimic focal tumor. Uptake in adrenals may be prominent

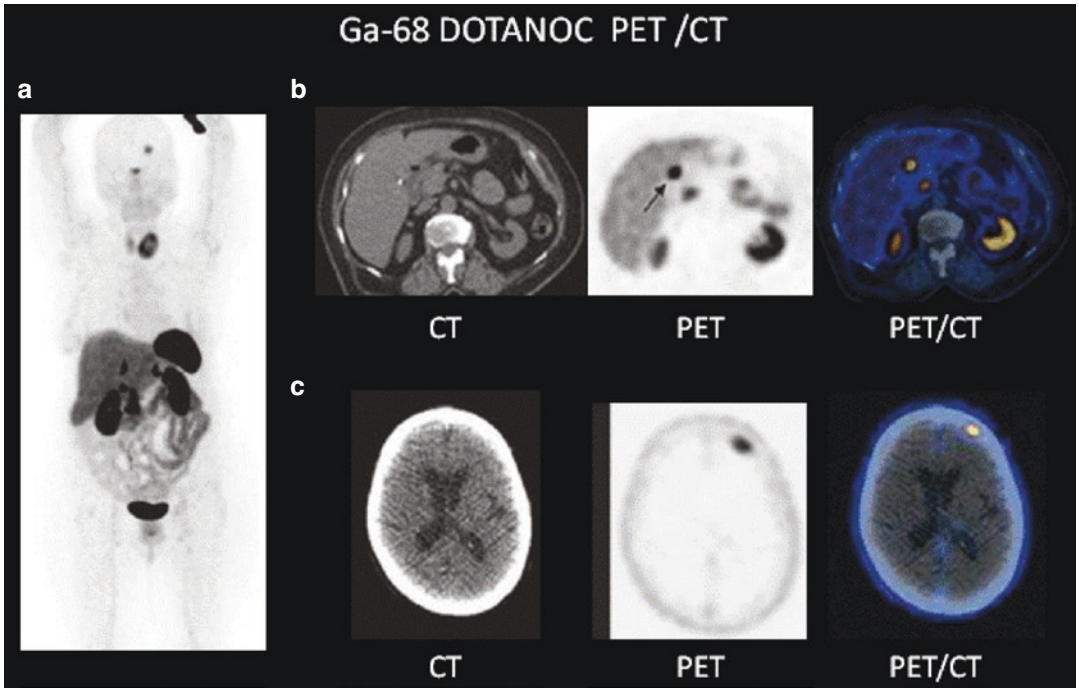

Fig. 6.24 Scintigraphic studies for a 74-year-old woman with duodenal 1 cm polyp, grade 1 carcinoid tumor, for staging. Ga-68 DOTANOC PET/CT whole-body MIP (**a**) and selected transaxial CT, PET, and PET/CT fusion images of the abdomen (**b**) and head (**c**) are shown. There is a focal uptake in the duodenal carcinoid (arrow) which is higher than liver activity. Incidentally, focal uptake is also seen in the left frontal region due to benign meningioma and markedly and heterogeneously increased uptake in the enlarged left thyroid lobe which can be due to medullary thyroid carcinoma, well-differentiated thyroid carcinoma, or carcinoid metastases. Physiological uptake is seen in the pituitary gland, right thyroid lobe, liver, spleen, both adrenal glands, pancreatic head, and bowel with excreted activity in the kidneys and bladder

References

1. Nurunnabi ASM, Alim A, Sabiha M, Manowara B, Monira K, Shamim A (2010) Weight of the human thyroid gland: a postmortem study. Bangladesh J Med Sci 9(1):44–48
2. Ellis H (2007) Anatomy of the thyroid and parathyroid glands. Surgery 25(11): 467–468
3. Sarkar SD (1996) Thyroid pathophysiology. In: Sandler MP, Coleman RE, FJ TW (eds) Diagnostic nuclear medicine. Williams and Wilkins, Baltimore, pp 899–909
4. Cooper DS (2005) Antithyroid drugs. N Engl J Med 352:905–917
5. Malozowski S, Chiesa A (2010) Propylthiouracil-induced hepatotoxicity and death. Hopefully, nevermore. J Clin Endocrinol Metab 95:3161–3163
6. Silberstein EB, Alavi A, Balon HR et al (2012) The SNM practice guideline for therapy of thyroid disease with 131I. J Nucl Med 53
7. Sarkar SD, Savitch I (2004) Management of thyroid cancer. Appl Radiol 33:34–45
8. Tala H, Robbins R, Fagin JA et al (2011) Five-year survival is similar in thyroid cancer patients with distant metastases prepared for radioactive iodine therapy with either thyroid hormone withdrawal or recombinant human TSH. J Clin Endocrinol Metab 96:2105–2111
9. Sarkar SD, Afriyie MO, Palestro CJ (2001) Recombinant human thyroid-stimulating-hormone-aided scintigraphy: comparison of imaging at multiple times after I-131 administration. Clin Nucl Med 26:392–395
10. Moog F, Linke R, Manthey N et al (2000) Influence of thyroid stimulating hormone levels on uptake of FDG in recurrent and metastatic differentiated thyroid carcinoma. J Nucl Med 41:1989–1995
11. Akamizu T, Satoh T, Isozaki O et al (2012) Diagnostic criteria, clinical features, and incidence of thyroid storm based on nationwide surveys. Thyroid 22:661–679

12. Chin BB, Patel P, Cohade C et al (2004) Recombinant human thyrotropin stimulation of fluoro-D-glucose positron emission tomography in well-differentiated thyroid carcinoma. J Clin Endocrinol Metab 89:91–95
13. Bidart JM, Mian C, Lazar V, Russo D, Filetti S, Caillou B et al (2000) Expression of pendrin and the Pendred syndrome (PDS) gene in human thyroid tissues. J Clin Endocrinol Metab 2000(85):2028–2033
14. Mitchell AM, Manley SW, Morris JC, Powell KA, Bergert ER, Mortimer RH (2001) Sodium iodide symporter (NIS) gene expression in human placenta. Placenta 22:256–258
15. Pearce EN, Lazarus JH, Moreno-Reyes R, Zimmermann MB (2016) Consequences of iodine deficiency and excess in pregnant women: an overview of current knowns and unknowns. Am J Clin Nutr 104:918S–923S
16. Koukkou EG, Roupas ND, Markou KB (2017) Effect of excess iodine intake on thyroid on human health. Minerva Med 108:136–146
17. Bogazzi F, Bartalena L, Gasperi M et al (2001) The various effects of amiodarone on thyroid function. Thyroid 11:511–519
18. Daniels GH (2001) Amiodarone-induced thyrotoxicosis. J Clin Endocrinol Metab 86:3–8
19. Laurie AJ, Lyon SG, Lasser EC (1992) Contrast material iodides: potential effects on radioactive iodine thyroid uptake. J Nucl Med 33:237–238
20. Sarkar SD, Kalapparambath T, Palestro CJ (2002) Comparison of I-123 and I-131 for whole body imaging in thyroid cancer. J Nucl Med 43:632–634
21. Ward LS, Santarosa PL, Granja F et al (2003) Low expression of sodium iodide symporter identifies aggressive thyroid tumors. Cancer Lett 200:85–91
22. Bertagna F, Treglia G, Piccardo G et al (2012) Diagnostic and clinical significance of F-18-FDG-PET/CT thyroid incidentalomas. J Clin Endocrinol Metab 97:3866–3875
23. Castellana M, Trimboli P, Piccardo A, Giovanella L, Treglia G (2019) Performance of 18F-FDG PET/CT in selecting thyroid nodules with indeterminate fine-needle aspiration cytology for surgery. A systematic review and a meta-analysis. J Clin Med 8:1333
24. Kim YH, Chang Y, Kim Y, Kim SJ, Rhee EJ et al (2019) Diffusely increased 18F-FDG uptake in the thyroid gland and risk of thyroid dysfunction: a cohort study. J Clin Med 8:443
25. Padma V, Ramakrishnan C (2019) Malignancy in solitary thyroid nodules: a study on incidence & evaluation of risk. Indian J Public Health Res Dev 10:4253–4255
26. Kishan AM, Prasad K (2018) Prevalence of solitary thyroid nodule and evaluation of the risk factors associated with occurrence of malignancy in a solitary nodule of thyroid. Int Surg J 5(6):2279–2285
27. Guth S, Theune U, Aberle J, Galach A, Bamberger CM (2009) Very high prevalence of thyroid nodules detected by high frequency (13 MHz) ultrasound examination. Eur J Clin Investig 39:699–706
28. Jiang H, Tian Y, Yan W, Kong Y, Wang H, Wang A et al (2016) The prevalence of thyroid nodules and an analysis of related lifestyle factors in Beijing communities. Int J Environ Res Public Health 13:1–11
29. Holm LE, Blomgren H, Lowhagen T (1985) Cancer risks in patients with chronic autoimmune thyroiditis. N Engl J Med 312:601–604
30. Belfiore A, La Rosa GL, La Porta GA, Giuffrida D, Milazzo G, Lupo L et al (1992) Cancer risk in patients with cold thyroid nodules: relevance of iodine intake, sex, age, and multinodularity. Am J Med 93:363–369
31. Fabrizio Monaco F (2003) Classification of thyroid diseases: suggestions for a revision. J Clin Endocrinol Metabol 88:1428–1432
32. Fernandez-Soto L, Gonzalez A, Escobar-Jimenez F et al (1998) Increased risk of autoimmune thyroid disease in hepatitis C vs hepatitis B before, during, and after discontinuing interferon therapy. Arch Intern Med 158:1445–1448
33. Hooft L, Hoekstra OS, Deville W et al (2001) Diagnostic accuracy of ^{18}F-fluorodeoxyglucose positron emission tomography in the follow-up of papillary or follicular thyroid cancer. J Clin Endocrinol Metab 86:3779–3786
34. Sarkar SD, Becker DV (1995) Thyroid uptake and imaging. In: Becker KL (ed) Principles and practice of endocrinology and metabolism. Lippincott, Philadelphia, pp 307–313
35. Dang AH, Hershman JM (2002) Lithium-associated thyroiditis. Endocr Pract 8:232–236
36. Amino N, Tada H, Hidaka Y et al (1999) Screening for postpartum thyroiditis. J Clin Endocrinol Metab 84:1813
37. Stagnaro-Green A (2002) Postpartum thyroiditis. J Clin Endocrinol Metab 87:4042–4047
38. Premawardhana LDKE, Parkes AB, John R et al (2004) Thyroid peroxidase antibodies in early pregnancy: utility for prediction of postpartum thyroid dysfunction and implications for screening. Thyroid 14:610–615
39. Mandac JC, Chaudhry S, Sherman KE, Tomer Y (2006) The clinical and physiological spectrum of interferon-alpha induced thyroiditis: toward a new classification. Hepatology 43(4):661–672
40. Oppenheim Y, Ban Y, Tomer Y (2004) Interferon induced autoimmune thyroid disease (AITD): a model for human autoimmunity. Autoimmun Rev 3:388–393
41. Bliddal S, Nielsen CH, Feldt-Rasmussen U (2017) Recent advances in understanding autoimmune thyroid disease: the tallest tree in the forest of polyautoimmunity. F1000 Res 6:1776. https://doi.org/10.12688/f1000research.11535.1
42. Vestergaard P, Rejnmark L, Weeke J et al (2002) Smoking as a risk factor for Graves' disease, toxic nodular goiter, and autoimmune hypothyroidism. Thyroid 12:69–75

43. Fountoulakis S, Tsatsoulis A (2004) On the pathogenesis of autoimmune thyroid disease: a unifying hypothesis. Clin Endocrinol 60:397–409
44. Li Y, Teng D, Shan Z et al (2008) Antithyroperoxidase and antithyroglobulin antibodies in a five-year follow up survey of populations with different iodine intakes. J Clin Endocrinol Metab 93:1751–1757
45. Nygaard B, Knudsen JH, Hegedus L et al (1997) Thyrotropinreceptor antibodies and Graves' disease, a side-effect of I-131 treatment in patients with nontoxic goiter. J Clin Endocrinol Metab 82:2926–2930
46. Surks MI, Ortiz E, Daniels GH et al (2004) Subclinical thyroid disease: scientific review and guidelines for diagnosis and management. JAMA 291:228–238
47. Weetman AP (2000) Graves disease. N Engl J Med 343:1236–1248
48. Ahmed A, Craig W, Krukowski ZH (2012) Quality of life after surgery for Graves' disease: comparison of those having surgery intended to preserve thyroid function with those having ablative surgery. Thyroid 22:494–500
49. Burch HB, Burman KD, Cooper DS (2012) A 2011 survey of clinical practice patterns in the management of Graves' disease. J Clin Endocrinol Metab 97:4549–4558
50. La Vecchia C, Malvezzi M, Bosetti C, Garavello W, Bertuccio P, Levi F, Negri E (2015) Thyroid cancer mortality and incidence: a global overview. Int J Cancer 136:2187–2195
51. Tumino D, Grani G, Di Stefano M, Di Mauro M, Scutari M et al (2020) Nodular thyroid disease in the era of precision medicine. Front Endocrinol 10:907
52. Elgazzar AH, Alenezi S, Alshammari JM, Ghanem M, Asa'Ad S (2015) Value of oblique view in nodular thyroid disease; revisiting fundamentals. World J Nucl Med 14:125
53. Liu Y (2009) Clinical significance of thyroid uptake on F18-fluorodeoxyglucose positron emission tomography. Ann Nucl Med 23:17–23
54. Soto GD, Halperin I, Squarcia M, Lomeña F, Domingo MP (2010) Update in thyroid imaging. The expanding world of thyroid imaging and its translation to clinical practice. Hormones 9:287–298
55. Sarkar SD (2006) Benign thyroid disease: what is the role of nuclear medicine? Semin Nucl Med 36:185–193
56. Bath SC, Steer CD, Golding J, Emmett P, Rayman MP (2013) Effect of inadequate iodine status in UK pregnant women on cognitive outcomes in their children: results from the Avon Longitudinal Study of Parents and Children (ALSPAC). Lancet 382:331–337
57. Hynes KL, Otahal P, Burgess JR, Oddy WH, Hay I (2017) Reduced educational outcomes persist into adolescence following mild iodine deficiency in utero, despite adequacy in childhood: 15-year follow-up of the Gestational Iodine Cohort investigating auditory processing speed and working memory. Nutrients 9:pii:E135477
58. Abel MH, Caspersen IH, Meltzer HM, Haugen M, Brandlistuen RE, Aase H, Alexander J, Torheim LE, Brantsaeter AL (2017) Suboptimal maternal iodine intake is associated with impaired child neurodevelopment at 3 years of age in the Norwegian mother and child cohort study. J Nutr 147:1314–1324
59. Levie D, Tim I, Korevaar M, Bath SC, Dalmau-Bueno A et al (2018) Thyroid function in early pregnancy, child IQ, and autistic traits: a meta-analysis of individual participant data. J Clin Endocrinol Metabol 103:2967–2297
60. Taterra D, Wong LM, Vikse J, Sanna B, Pękala P, Walocha J, Cirocchi R, Tomaszewski K, Henry BM (2019) The prevalence and anatomy of parathyroid glands: a meta-analysis with implications for parathyroid surgery. Langenbeck's Arch Surg 404(1):63–70. 55
61. Alenezi SA, Asa'ad SM, Elgazzar AH (2015) Scintigraphic parathyroid imaging: concepts and new developments. Res Rep Nucl Med 5:9–18
62. Quiros RM, Warren W, Prinz RA (2004) Excision of a mediastinal parathyroid gland with use of video-assisted thoracoscopy, intraoperative 99mTc-sestamibiscanning, and intraoperative monitoring of intact parathyroid hormone. Endocr Pract 10:45–48
63. Taterra D, Wong LM, Vikse J, Sanna B, Pękala P, Walocha J et al (2019) The prevalence and anatomy of parathyroid glands: a meta-analysis with implications for parathyroid surgery. Langenbeck's Arch Surg 404:63–70
64. Akerstrom G, Grimelius L, Johansson H, Lundquist H, Pertoft H, Bergstrom R (1981) The parenchymal cell mass in normal human parathyroid glands. Acta Pathol Microbiol Immunol Scand 89(A):367
65. Akerstrom G, Rudberg C, Grimelius L et al (1986) Histologic parathyroid abnormalities in an autopsy series. Hum Pathol 17:520–527
66. Heath H III (1991) Clinical spectrum of primary hyperparathyroidism: evolution with changes in medical practice and technology. J Bone Mineral Res 6:S63–S70
67. Bilezikian JP, Bandeira L, Khan A, Cusano NE (2018) Hyperparathyroidism. Lancet 391(10116):168–178
68. Silva BC, Cusano NE, Bilezikian JP (2018) Primary hyperparathyroidism. Best Pract Res Clin Endocrinol Metab 32(5):593–607
69. Yeh MW, Ituarte PHG, Zhou HC et al (2013) Incidence and prevalence of primary hyperparathyroidism in a racially mixed population. J Clin Endocrinol Metab 98(3):1122–1129
70. Ljunghall S, Hellman P, Rastad J, Akerström G (1991) Primary hyperparathyroidism: epidemiology, diagnosis and clinical picture. World J Surg 15(6):681–687
71. Herfarth KK, Wells SA (1997) Parathyroid glands and the multiple endocrine neoplasia syndromes and familial hypocalciuric hypercalcemia. Semin Surg Oncol 13:114–124
72. Duh QY, Hybarger CP, Geist R, Gamsu G, Goodman PC, Gooding GA, Clark OH (1987) Carcinoids asso-

ciated with multiple endocrine neoplasia syndromes. Am J Surg 154:142–148
73. Beus KS, Stack BC (2004) Synchronous thyroid pathology in patients presenting with primary hyperparathyroidism. Am J Otolaryngol 25:308–312
74. Sidhu S, Campbell P (2000) Thyroid pathology associated with primary hyperparathyroidism. Aust NZJ Surg 70:285–287
75. Hedman IL, Tisell LE (1984) Associated hyperparathyroidism and non-medullary thyroid carcinoma: the etiological role of radiation. Surgery 95:392–397
76. Lau WL, Obi Y, Kalantar-Zadeh K (2018) Parathyroidectomy in the management of secondary hyperparathyroidism. Clin J Am Soc Nephrol 13(6):952–961
77. Thompson NW, Eckhauser FE, Harness JK (1982) The anatomy of primary hyperparathyroidism. Surgery 92:814–821
78. Simeone DM, Sandelin K, Thompson NW (1995) Undescended superior parathyroid gland: a potential cause of failed cervical exploration for hyperparathyroidism. Surgery 118:949–956
79. Tezelman S, Shen W, Shaver JK et al (1993) Double parathyroid adenomas: clinical and biochemical characteristics before and after parathyroidectomy. Ann Surg 218:300–309
80. Bartsch D, Nies C, Hasse C et al (1995) Clinical and surgical aspects of double adenoma in patients with primary hyperparathyroidism. Br J Surg 82:926–929
81. Nguyen BD (1999) Parathyroid imaging with Tc-99msestamibiplanar and SPECT scintigraphy. Radiographics 19:601–614
82. Clark OH, Duh QY (1989) Primary hyperparathyroidism: a surgical perspective. Endocrinol Metab Clin N Am 18:701–714
83. McHenry CR, Lee K, Saadey J et al (1996) Parathyroid localization with technetium-99m-sestamibi: a prospective evaluation. J Am Coll Surg 183:25–30
84. Bergenfelz A, Tennvall J, Valdermarsson S et al (1997) Sestamibiversusthallium subtraction scintigraphy in parathyroid localization: a prospective comparative study in patients with predominantly mild primary hyperparathyroidism. Surgery 121:601–605
85. Rogers LA, Fetter BF, Peete WPJ (1969) Parathyroid cyst and cystic degeneration of parathyroid adenoma. Arch Pathol 88:476–479
86. Fallon MD, Haines JW, Teitelbaum SL (1982) Cystic parathyroid gland hyperplasia-hyperparathyroidism presenting as a neck mass. Am J Clin Pathol 77:104–107
87. Turner WJD, Baergen RN, Pellitteri PK, Orloff LA (1996) Parathyroid lipoadenoma: case report and review of the literature. Otolaryngol Head Neck Surg 114:313–316
88. Cummings CW (2005) Otolaryngology: head and neck surgery, 4th edn. Mosby, Philadelphia
89. Cheng L, Bostwick DG (2011) Endocrine pathology. In: Essentials of anatomic pathology, 3rd edn. Springer, Berlin, pp 927–928
90. Rinsho N (1995) Primary hyperparathyroidism, pathologic findings and ultrastructure. Jpn J Clin Med 53:861–863
91. Chen CC, Premkumar A, Hill SC, Skarulis MC, Spiegel AM (1995) Tc-99msestamibi imaging of a hyperfunctioning parathyroid autograft with Doppler ultrasound and MRI correlation. Clin Nucl Med 20:222–225
92. Lee VS, Spritzer CE, Coleman RE, Wilkinson RH Jr, Coogan AC, Leight GS Jr (1995) Hyperparathyroidism in high-risk surgical patients: evaluation with double-phase technetium-99msestamibiimaging. Radiology 197:627–633
93. Walker RP, Paloyan E, Gopalsami C (2004) Symptoms in patients with primary hyperparathyroidism: muscle weakness or sleepiness. Endocr Pract 10:404–408
94. Wang CA (1977) Parathyroidre-exploration: a clinical and pathological study of 112 cases. Ann Surg 186:140
95. Assalia A, Inabnet WB (2004) Endoscopicparathyroidectomy. Otolaryngol Clin N Am 37:871–886
96. O'Doherty MJ, Kettle AG (2003) Parathyroid imaging: preoperative localisation. Nucl Med Commun 24:125–131
97. Mitchell BK, Merrell RC, Kinder BK (1995) Localization studies in patients with hyperparathyroidism. Endocr Surg 75:483–498
98. Kao A, Shiau YC, Tsai SC, Wang JJ, Ho ST (2002) Technetium-99mmethoxyisobutylisonitrile imaging for parathyroid adenoma: relationship to P-glycoprotein or multidrug resistance-related protein expression. Eur J Nucl Med Mol Imaging 29:1012–1015
99. Goris ML, Basso LV, Keeling C (1991) Parathyroid imaging. J Nucl Med 32:887–889
100. O'Doherty MJ, Kettle AG, Wells P, Collins RE, Coakley AJ (1992) Parathyroid imaging with technetium99m-sestamibi: preoperative localization and tissue up take studies. J Nucl Med 33: 313–318
101. Takebayashi S, Hidai H, Chiba T, Takaga Y, Nagatani Y, Matsubara S (1999) Hyper functional parathyroid glands with Tc-99mMIBI scan: semiquantitative analysis correlated with histologic findings. J Nucl Med 40:1792–1797
102. Sandrock D, Merino MJ, Norton JA, Neumann RD (1993) Ultrastructural histology correlates with results of thallium-201/technetium-99m parathyroid subtraction scintigraphy. J Nucl Med 34:24–29
103. Naddaf S, Anim JJ, Farghaly MM, Behbehani AE, Alshomar KA, Elgazzar AH (2004) Ultrastructure of hyperfunctioning parathyroid glands: does it explain various patterns of sestamibi uptake. Proceedings of the 9th annual Health science poster day and conference, Kuwait, April 19–21, p 61
104. Dontu VS, Kettle AG, O'Doherty MJ, Coakley AJ (2004) Optimization of parathyroid imaging by simultaneous dual energy planar and single pho-

ton emission tomography. Nucl Med Commun 25:1089–1093
105. Melton GB, Somervell H, Friedman KP, Zeiger MA, Cahid CA (2005) Interpretation of ^{99m}Tcsestamibiparathyroid SPECT scan is improved when read by the surgeon and nuclear medicine physician together. Nucl Med Commun 26:633–638
106. Parikh AM, Suliburk JW, Morón FE (2018) Imaging localization and surgical approach in the management of ectopic parathyroid adenomas. Endocr Pract 24(6):589–598
107. Takahashi H et al (2013) Fusion images of MIBISPECT and MDCT improved iagnostic performance of localization study in hyperparathyroidism with multigland disease. J Nucl Med 54:44
108. Zeng M, Liu W, Zha X, Tang S, Liu J, Yang G et al (2019) 99mTc-MIBI SPECT/CT imaging had high sensitivity in accurate localization of parathyroids before parathyroidectomy for patients with secondary hyperparathyroidism. Ren Fail 41(1):885–892
109. Beggs AD, Hain SF (2005) Localization of parathyroid adenomas using ^{11}C-methionine positron emission tomography. Nucl Med Commun 26:133–136
110. Broos WA, Wondergem M, Knol RJ, van der Zant FM (2019) Parathyroid imaging with 18 F-fluorocholine PET/CT as a first-line imaging modality in primary hyperparathyroidism: a retrospective cohort study. EJNMMI Res 9:1–7
111. Erickson LA (2014) Adrenal gland histology. In: Atlas of endocrine pathology. Springer, New York, NY, pp 147–153
112. Aron DC, Tyrrell JB (1997) Glucocorticoids and adrenal androgens. In: Greenspan FS, Strewler GJ (eds) Basic and clinical endocrinology, 5th edn. Appleton and Lange, Norwalk, p 318
113. Goldfien A (1997) Adrenal medulla. In: Greenspan FS, Strewler GJ (eds) Basic and clinical endocrinology, 5th edn. Appleton and Lange, Norwalk, p 382
114. Ryan JJ, Rezkalla MA, Rizk SN, Peterson KG, Wiebe RH (1995) Testosterone-secreting adrenal adenoma that contained crystalloids of Reinke in an adult female patient. Mayo Clin Proc 70:380–383
115. Lynn MD, Gross MD, Shapiro B, Bassett D (1986) The influence of hypercholesterolemia on the adrenal uptake and metabolic handling of I-1316β-iodomethyl-19-norcholesterol(NP-59). Nucl Med Commun 1:631–635
116. Hedeland H, Ostberg G, Hokfelt B (1968) On the prevalence of adrenocortical adenomas in an autopsy material in relation to hypertension and diabetes. Acta Med Scand 184:211–214
117. Copeland PM (1983) The incidentally discovered adrenal mass. Ann Intern Med 98:940–945
118. Vos EL, Grewal RK, Russo AE, Reidy-Lagunes D, Untch BR, Gavane SC et al (2020) Predicting malignancy in patients with adrenal tumors using 18F-FDG-PET/CT SUVmax. J Surg Oncol 122(8):1821–1826
119. Volpe C, Enberg U, Sjögren A et al (2008) The role of adrenal scintigraphy in the preoperative management of primary aldosteronism. Scand J Surg 97:248–253
120. Evangelista L, DeFalco T, di Nuzzo C et al (2008) Utility of adrenal cortical scintigraphy with I-6-$-methyl-131 norcholesterol in a case of mismatch between morphological and functional PET imaging. Thyroid Sci 3:CR1–CR3
121. Omura M, Saito J, Yamaguchi K, Kakuta Y, Nishikawa T (2004) Prospective study on the prevalence of secondary hypertension among hypertensive patients visiting a general outpatient clinic in Japan. Hypertens Res 27:193–202
122. Huether SE, Tomky D (1998) Alterations of hormonal regulation. In: McCance KL, Huether SE (eds) Pathophysiology, the biologic basis for disease in adults and children, 3rd edn. Mosby, St Louis, p 700
123. Spencer RP (1998) Tumor-seeking radiopharmaceuticals: nature and mechanisms. In: Murray IP, Ell PJ (eds) Nuclear medicine in clinical diagnosis and treatment, 2nd edn. Churchill Livingstone, Hong Kong, p 764
124. Elgazzar AH, Gelfand MJ, Washburn LC, Clark J, Nagaraj N, Cummings D, Hughes J et al (1995) I-123MIBGscintigraphy in adults, are port of clinical experience. Clin Nucl Med 20:147
125. Gelfand MJ, Elgazzar AH, Kriss VM, Masters PR, Golsch GJ (1994) Iodine-123MIBGSPECT versus planar imaging in children with neural crest tumors. J Nucl Med 35:1753–1756
126. Parisi MT, Sandler ED, Hattner RS (1992) The biodistribution of metaiodobenzylguanidine. Semin Nucl Med 22:46–48
127. Okuyama C, Ushijima Y, Kubota T, Yoshida T, Nakai T, Kobayashi K, Nishimura T (2003) 123I-Metaiodobenzyl guanidine up take in the nape of the neck of children: likely visualization of brown adipose tissue. J Nucl Med 44:1421–1425
128. Shapiro B, Copp JE, Sisson JC, Eyre PL, Wallis J, Beierwaltes WH (1985) Iodine-131metaiodobenzyl-guanidine in the locating of suspected pheochromocytoma: experience in 400 cases. J Nucl Med 26:576
129. Paltiel HJ, Gelfand MJ, Elgazzar AH, Washburn LC, Harris RE, Masters PR, Golsch GJ (1994) Neural crest tumors: I-123MIBG imaging in children. Radiology 190:118
130. Liu B, Servaes S, Zhuang H (2018) SPECT/CT MIBG imaging is crucial in the follow-up of the patients with high-risk neuroblastoma. Clin Nucl Med 43(4):232–238
131. Aboian MS, Huang SY, Hernandez-Pampaloni M, Hawkins RA, VanBrocklin HF, Huh Y et al (2021) 124I-MIBG PET/CT to monitor metastatic disease in children with relapsed neuroblastoma. J Nucl Med 62(1):43–47
132. Samim A, Tytgat GA, Bleeker G, Wenker S, Chatalic KL, Poot AJ et al (2021) Nuclear medicine imaging in neuroblastoma: current status and new developments. J Personal Med 11(4):270

133. Shalaby-Rana E, Majd M, Andrich MP, Movassaghi N (1997) In-111pentetreotidescintigraphy in patients with neuroblastoma. Comparison with I-131MIBG, N-Myconcogene amplification, and patient outcome. Clin Nucl Med 22:315–319
134. Kropp J, Hofmann M, Bihl H (1997) Comparison of MIBG and pentetreotidescintigraphy in children with neuroblastoma. Is the expression of somatostatin receptors aprognostic factor? Anticancer Res 17:1583–1588
135. Tenenbaum F, Lumbroso J, Schlumberger M, Mure A, Plouin PF, Caillou B, Parmentier C (1995) Comparison of radiolabeled octreotide and metaiodobenzylguanidine (MIBG) scintigraphy in malignant pheochromocytoma. J Nucl Med 36:1–6
136. Pashankar FD, O'Dorisio MS, Menda Y (2005) MIBG and somatostatin receptor analogs in children: current concepts on diagnostic and therapeuticuse. J Nucl Med 46(Suppl 1):55S–61S
137. Manil L, Edeline V, Jlumbroso J, Lequen H, Zucker JM (1996) Indium-111-pentetreotidescintigraphy in children with neuroblast-derived tumors. J Nucl Med 37:893–896
138. Krausz Y, Keidar Z, Kogan I, Even-Sapir E, Bar-Shalom R, Engel A, Rubinstein R et al (2003) SPECT/CT hybrid imaging with ^{111}In-pentetreotide in assessment of neuroendocrine tumours. Clin Endocrinol 59:565–573
139. Andersson P, Forssel-Aronsson E, Johanson V, Wangberg B, Nilsson O, Fjalling M, Ahlman H (1996) Internalization of indium-111intohuman neuroendocrine tumor cells after incubation with indium-111-DTPA-D-Phe1-Octreotide. J Nucl Med 37:2002–2006
140. Andersson P, Forssel-Aronsson E, Johanson V, Wangberg B, Nilsson O, Fjalling M, Ahlman H (1996) Internalization of indium-111 into human neuroendocrine tumor cells after incubation with indium-111-DTPA-D-Phe 1-octreotide. J Nucl Med 37:2002–2200
141. Trampal C, Engler H, Juhlin C, Bergstrom M, Langstrom B (2004) Pheochromocytomas: detection with C-11hydroxyephedrine PET. Radiology 230:423–428
142. Ruf J, Hueck F, Schiefer J, Denecke T, Elgeti F et al (2010) Impact of multiphase 68Ga-DOTATOC-PET/CT on therapy management in patients with neuroendocrine tumors. Neuroendocrinology 91:101–109
143. Ilias I, Yu J, Carrasquillo JA, Chen CC, Eisenhofer G, Whatley M, McElroy B et al (2003) Superiority of 6-[18F]-fluorodopamine positron emission tomography versus [131I]-metaiodobenzylguanidinescintigraphy in the localization of metastatic pheochromocytoma. J Clin Endocrinol Metab 88:4083–4087
144. Brunt LM, Moley JF (2001) Adrenal incidentaloma. World J Surg 25:905–913
145. Mantero F, Masini AM, Opocher G, Giovagnetti M, Arnaldi G (1997) Adrenal incidentaloma: an overview of hormonal data from the National Italian Study Group. Horm Res 47:284–289
146. Minn H, Salonen A, Friberg J, Roivainen A, Viljanen T, Langsjo J, Salmi J et al (2004) Imaging of adrenal incidentalomas with PET using C-11metomidate and 18F-FDG. J Nucl Med 45:972–979
147. Khan TS, Sundin A, Juhlin C, Langstrom B, Bergström M, Eriksson B (2003) 11C-metomidatePET imaging of adrenocortical cancer. Eur J Nucl Med Mol Imaging 30:403–410
148. Rubello D, Bui C, Casara D et al (2002) Functional scintigraphy of the adrenal gland. Eur J Endocrinol 147:13–28
149. Akkuş G, Güney IB, Ok F, Evran M, Izol V et al (2019) Diagnostic efficacy of 18F-FDG PET/CT in patients with adrenal incidentaloma. Endocr Connect 8:838–845